ACTINIDE RESEARCH QUARTERLY

Los Alamos National Laboratory

Issue 2 • August 2013

89 Ac 90 Th 91 Pa 92 U 93 Np 94 Pu 95 Am 96 Cm 97 Bk 98 Cf 99 Es 100 Fm 101 Md 102 No 103 Lr

2012 Plutonium Futures Conference Issue

Contribution by the 2012 Conference Co-Chairs
David Geeson, AWE
Thomas Fanghaenel, JRC-ITU
Claude Guet, CEA

Los Alamos National Laboratory, an affirmative action/equal opportunity employer, is operated by Los Alamos National Security, LLC, for the National Nuclear Security Administration of the U.S. Department of Energy under contract DE-AC52-06NA25396.

This publication was prepared as an account of work sponsored by an agency of the U.S Government. Neither Los Alamos National Security, LLC, the U.S. Government nor any agency thereof, nor any of their employees make any warranty, express or implied, or assume any legal liability or responsibility for the accuracy, completeness, or usefulness of any information, apparatus, product, or process disclosed, or represent that its use would not infringe privately owned rights. Reference herein to any specific commercial product, process, or service by trade name, trademark, manufacturer, or otherwise does not necessarily constitute or imply its endorsement, recommendation, or favoring by Los Alamos National Security, LLC, the U.S. Government, or any agency thereof. The views and opinions of authors expressed herein do not necessarily state or reflect those of Los Alamos National Security, LLC, the U.S. Government, or any agency thereof. Los Alamos National Laboratory strongly supports academic freedom and a researcher's right to publish; as an institution, however, the Laboratory does not endorse the viewpoint of a publication or guarantee its technical correctness.

LA-UR-13-26941

This issue of the Actinide Research Quarterly (ARQ) revisits the 2012 Plutonium Futures–The Science Conference that took place at Cambridge University July 15–20. The iconic architecture made a dramatic backdrop for the conference, which was the seventh in a series of important international conferences that was initiated in 1997 to provide an international forum for the presentation and discussion of current research on physical and chemical properties and environmental interactions of plutonium and other actinides. It also addresses the technical basis of a number of health, safety, and security issues relating to the actinides that merit significant national and international attention, including the safe storage and long-term management of surplus weapons materials as well as the management of large inventories of actinides from civilian nuclear power generation.

The technical themes for the Plutonium Futures 2012 Conference spanned condensed matter physics; detection and analysis; materials science; nuclear fuel cycle; and environmental behavior. It was hosted by the Atomic Weapons Establishment (AWE, United Kingdom), the Alternative Energies and Atomic Energy Commission (CEA, France), the European Commission Joint Research Centre–Institute for Transuranium Elements (ITU, Germany), and the National Nuclear Laboratory (NNL, United Kingdom) Sponsors were The Worshipful Company of Armourers and Braziers, the Royal Society of Chemistry, the Institute of Physics, and the Institute of Materials, Minerals and Mining. Nearly 250 delegates were attracted from 18 countries contributing 82 oral and 130 poster presentations.

Each oral session had two themes running in parallel and was preceded by a single plenary session bringing the whole delegate base together. The poster sessions were held over three days and spanned the lunch breaks with delegates participating in a buffet lunch while engaging with the poster presenters. The Tuesday evening highlight was a topical lecture on "The Impact of the 2011 Fukushima Nuclear Accident" delivered by Dr. Mike Weightman, UK Chief Inspector of Nuclear Installations, which attracted much interest and debate. The conference dinner was held in the Queens' College dining hall, a spectacular example of Cambridge dining in the 15th century college founded by Margaret of Anjou (Queen of Henry VI) and site of the famous Mathematical Bridge over the river Cam. After a well-earned dinner, delegates were entertained with some anecdotes and reflections from Prof. Roger Cashmore.

The week previous to the main conference included an Actinet-sponsored Summer School hosted by the NNL and held in Whitehaven, Cumbria. Forty young delegates were tutored by 14 leading researchers in a wide range of research fields including materials science, the nuclear fuel cycle, and condensed matter physics. Accompanying site visits were made to several parts of the civilian nuclear complex at the Sellafield site on the Cumbrian coastline.

Plutonium Futures–The Science Conference 2014 returns to the United States where it will be held at the Renaissance Hotel in Las Vegas, Nevada from September 7–11. See last page for more details.

Table of Contents

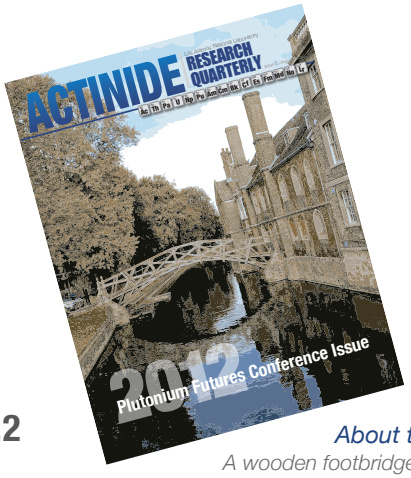

About the cover:
A wooden footbridge spans the River Cam, connecting two parts of Queens' College, University of Cambridge, site of Pu Futures 2012. The sophisticated mathematical design gives an arched appearance using only straight timbers. The design, first developed in 1749, is used for two bridges across the Cam. The conference logo was an interpretation of this form.

Introduction
2012 Conference Co-Chairs: David Geeson, Atomic Weapons Establishment (United Kingdom); Thomas Fanghaenel, European Commission, Joint Research Centre, Institute for Transuranium Elements; Claude Guet, Alternative Energies and Atomic Energy Commission (France)

Challenges for Future Plutonium Recycling: The French Vision.....2
Herve Bernard, Deputy CEO, Alternative Energies and Atomic Energy Commission (CEA) (France)

The Intriguing High-temperature Studies of Plutonium Dioxide and Mixed Oxide Solid Solutions.....7
Rudy J. M. Konings and Dario Manara of the European Commission, Joint Research Centre, Institute for Transuranium Elements; and Christine Gueneau, Alternative Energies and Atomic Energy Commission (France)

A New Focus for the United Kingdom's Civilian Nuclear Research and Development 12
John R. Beddington, Government Chief Scientific Adviser and chairman of the Nuclear Research and Development Advisory Board; Graham A. Fairhall, Chief Science and Technology Officer of the National Nuclear Laboratory; and Francis R. Livens, Research Director of the University of Manchester's Dalton Nuclear Institute

First Observation of Pu-239 Nuclear Magnetic Resonance.....16
Georgios Koutroulakis, Los Alamos National Laboratory; Hiroshi Yasuoka, Advanced Science Research Center, Japan Atomic Energy Agency

Safe and Secure Storage of Plutonium Dioxide in the United Kingdom.....20
Paul Cook of Sellafield Ltd; Howard Sims and David Woodhead, National Nuclear Laboratory

Alpha Decay in Plutonium, Radiogenic Helium, and Plutonium Swelling 28
Boris A. Nadykto, Russian Federal Nuclear Center

High-resolution Magic Angle Spinning Solid State Nuclear Magnetic Resonance Facility for Actinide-bearing Compounds 36
J. Somers, I. Farnan, L.Martel, O. Pauvert, C. Selfslag, T. Fanghanel, European Commission, Joint Research Centre, Institute for Transuranium Elements

Plutonium-rich Fast Reactor Spent Fuel Reprocessing in CORAL and Beyond.....40
R. Natarajan, V. Vijayakumar, V. Sundararaman, A. Ravisankar, Reprocessing Group, Indira Gandhi Centre for Atomic Research (India)

The Optical Properties of the Plutonium/Plutonium Oxide Thin Film System 47
David L. Pugmire, Franz J. Freibert, Joseph P. Baiardo, Los Alamos National Laboratory (US)

This article was contributed by Hervé Bernard, Deputy CEO, Alternative Energies and Atomic Energy Commission (CEA).

Challenges for Future Plutonium Recycling:

The French Vision

Introduction

Challenges imposed both by climate change and the coming era of fossil resource scarcity call for low-carbon technologies. France, for its part, firmly supports a mix of both nuclear and renewable energy. In this spirit, France proceeds in compliance with the European climate energy goals of 2020, as follow:

- Increase renewable energy sources to 23%
- Reduce greenhouse gas emissions by 20%
- Increase energy efficiency and awareness

In France, 50% of primary energy consumption still relies on fossil fuels. Such a massive use of fossil fuels is not sustainable because it has a strong, increasingly negative, impact on the environment, the climate, public health, and on the economies of many countries. France, for example, has no more fossil resources and must import fossil fuels at an always more expensive cost. Our 2011 fossil fuel imports represented an expense three times larger than in 2005 and constitute 90% of France's trade deficit.

For all these reasons, our top priority must be the substitution of fossil fuel with CO_2-free energy sources as soon as possible and as much as possible. Therefore, we need to develop alternative solutions, including energy savings and improved efficiency. The options are renewable and nuclear energies.

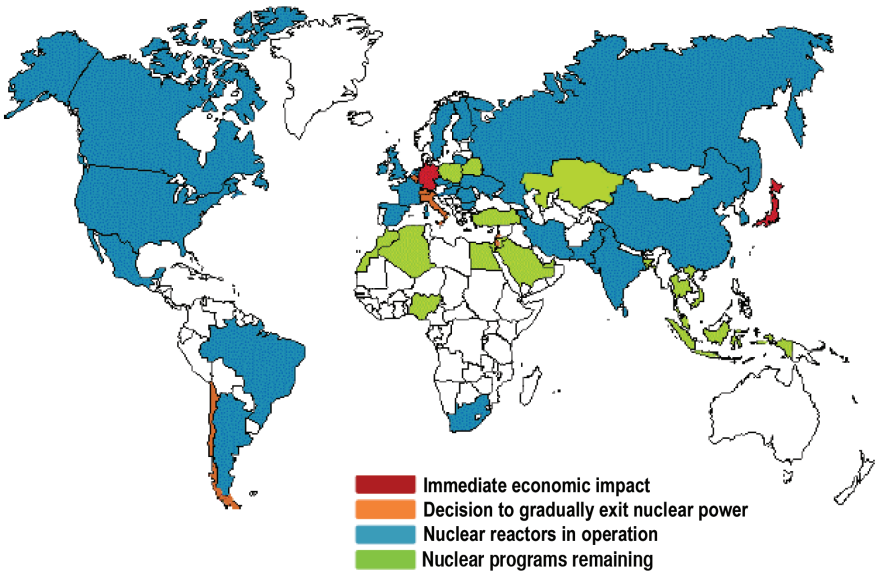

Figure 1. Countries' positions on nuclear power after the 2011 Fukushima accident.

The Nuclear Option

Even in the post-Fukushima context, the fundamental reasons justifying the nuclear option have not been modified. Although some countries have decided on, or are considering, a nuclear phase out, nuclear energy remains a widely shared choice (Fig. 1): some 60 nuclear power plants are currently under construction in the world. France has clearly confirmed its will to maintain the use of nuclear energy in order to preserve the country's economic competitiveness and the security of its energy supplies. France is also improving its nuclear technical and organizational safety measures to comply with the highest standards and considers it essential to regain public confidence in nuclear power throughout Europe and the world.

Reactors and closed fuel cycling, which offer the best safety features while staying economically competitive, have to be promoted in the future. The consequences of using plutonium (Pu) are at center stage of the French nuclear strategy and are the focus of research and development (R&D) programs in support of this technology. France chose Pu mono-recycling in light water reactors (LWR) more than 20 years ago and implemented it in the La Hague reprocessing plant. Fuel treatment and recycling require the following:

- Dissolving the spent nuclear fuel to access the nuclear materials
- Extracting the valuable elements, uranium (U) and Pu from mainly fission products (FP) and minor actinides.

The PUREX process is currently used to separate U and Pu. This process is based on the selective extraction of U(VI)-Pu(IV) by organic phase tri-butyl-phosphate (TBP) from other fission products that remain in the aqueous phase. The process is implemented by liquid-liquid extraction in counter-current devices such as pulsed columns or a centrifuge extractor in order to increase the effectiveness of separation (Fig. 2).

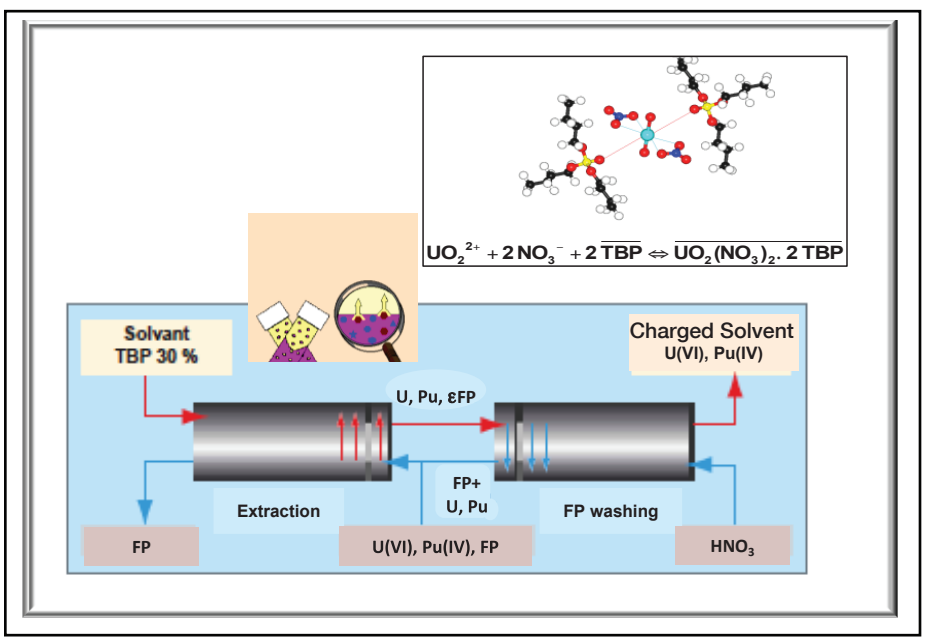

Figure 2. The PUREX process is based on the selective extraction of U(VI)-Pu(IV) by tri-butyl-phosphate (TBP).

In the La Hague plants, for example, both recovery yields and purification levels are very high; up to 99.9% of the U and Pu is recovered. A final conversion step allows production of oxide powders that are compatible with the specifications of the fuel fabrication process, thanks to the precipitation of intermediate oxalates. Recycling constitutes a significant improvement for waste management. It reduces the volume of the final waste by a factor of 5 and reduces its radiotoxicity by a factor of 10. The mono-recycling of plutonium in mixed oxide (MOX) fuel allows a savings of 17% of the uranium resources, with a very low impact on kilowatt hour (kWh) cost. It also allows the partial use of recycled and re-enriched uranium in UOx fuels.

The Alternative Energies and Atomic Energy Commission (CEA) is working with its industrial and academic partners to optimize the LWR fuel cycle. For example, the improvement for Pu mono-recycling is related to the implementation of the COEX™ process, which allows a complete comanagement of U and Pu, avoiding any pure Pu stockpile within the fuel cycle. It requires the coextraction of a (U, Pu) flux in the PUREX process and the subsequent production in the reprocessing plant of homogeneous $(U,Pu)O_2$ instead of pure PuO_2 powder.

Increasing resource consumption efficiency requires "fertilizing" ^{238}U by neutron capture and implementing Pu multirecycling in Generation IV fast neutron reactors, that are able to fully use the energetic potential of uranium resources; about a 100-fold improvement compared with LWRs. Reprocessing of fast reactor (FR) MOX fuels and subsequent Pu multirecycling have been demonstrated at the industrial scale in France. Twenty-seven tons of FR spent-MOX fuels have already been reprocessed in the APM (Marcoule) and UP2-400 (La Hague) plants in the 1980s and 1990s.

CEA is now implementing a large R&D program for more modern and efficient Pu recycling technologies. As decided by 2006 French legislation, the innovative sodium fast neutron demonstration reactor, Advanced Sodium Technological Reactor for Industrial Demonstration (ASTRID), should be built by 2020, and the CEA is strongly committed to the implementation of the supportive design and engineering programs. This effort includes studying applicable solutions that would continue to minimize the quantity and the toxicity of final highly radioactive waste. CEA is also making progress on the development of new minor actinide partitioning processes in support of their possible recycling, as tested in the Atalante facility (Marcoule).

Minor actinide recycling has been investigated at the CEA for the two last decades. Two options are considered: homogeneous and heterogeneous recycling. Homogeneous recycling aims to recover all the actinides; Pu, Am, and Cm, in a single flux, and then recycle Am and Cm at a low concentration (up to 2%) in all the fuel in the reactor core. Grouped actinides can be separated through the GANEX process (Group ActiNide EXtraction) with a goal of recovering all of the transuranium elements from the high-activity spent fuel solution. This process is in two steps: selective extraction of uranium and then partitioning of actinides from fission products

and lanthanides. Heterogeneous recycling recovers only the minor actinides Am and Cm in a dedicated flux. The actinides then are recycled in a specific target or blanket with a relatively high content (up to 20%) at the periphery of the reactor core.

Two processes were implemented: first, DIAMEX to coextract trivalent 4*f* and 5*f* elements, respectively lanthanides Ln(III) and actinides An(III); and second, SANEX, to selectively strip An(III) with a polyaminocarboxylate compound used in a buffered medium around pH=3.

A specific option of heterogeneous recycling would be to recycle only Am, since its contribution to the residual heat power and radiotoxicity is higher than that of Cm, and Am is easier to manage than Cm. This would simplify fuel manufacturing while allowing a subsequent potential benefit for a repository. The developed EXAm process is based on the extraction of Am, while Cm and other lanthanides remain in the aqueous phase. All the French separation processes described are based on liquid-liquid extraction. The processes benefit from the experience gained over the years by using the PUREX method in the La Hague plants.

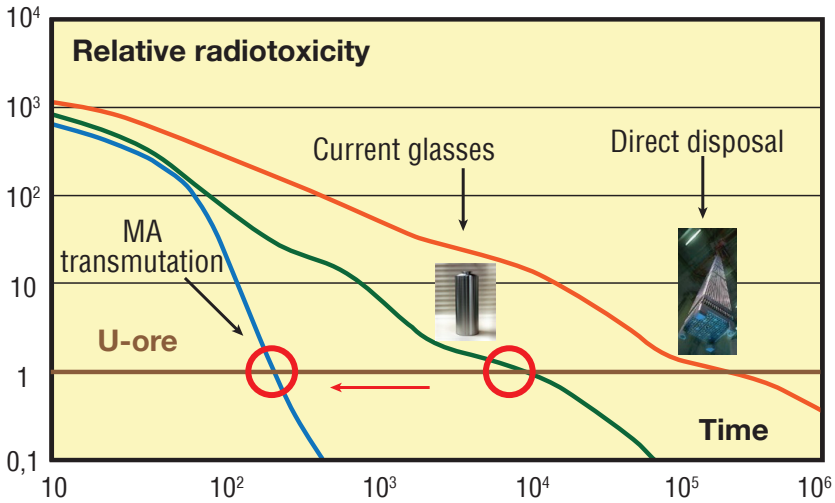

Figure 3. Graph shows length of time needed to reduce levels of radiotoxicity to that of uranium ore.

Recycling minor actinides would dramatically reduce the residual toxicity and the subsequent lifetime of the final waste (Fig. 3). Some hundreds of years would be sufficient to decrease the residual radiotoxicity down to that of natural uranium ore. Decreasing the waste heat power by recycling minor actinides, particularly americium, would also allow a denser repository and would significantly increase the waste volume to be stored in the same repository up to a factor of 8 (Fig. 4). The French geological repository will be defined in 2015 for already existing wastes with operation planned for 2025.

CEA also leads in R&D of many different kinds of fuel, such as oxide, carbide, nitride, or metal. Several different technologies are being studied. One is hydrometallurgy that produces powders to make pellets for the fuel pins. Also under study are two methods of pyrolysis: aggregates vibropacked in the fuel pins or metal-fuel casting. The cladding material for FR fuel is being investigated. Among others, oxide dispersed steels, are serious candidates because of their strong resistance to high irradiation dose.

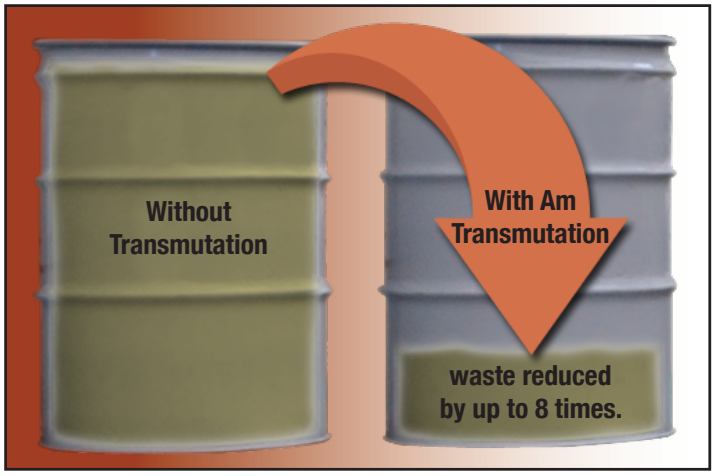

Figure 4. Denser waste repositories are made possible by recycling minor actinides.

Conclusion

Nuclear power has the potential to contribute even more in the future by using the Generation IV technologies. These technologies will enable the recycling of U and Pu and possibly minor actinides (mainly Am). Recycling actinides requires the development of fast reactors and the improvement of scientific knowledge on actinide basic chemistry and separation science.

In spite of the recent Fukushima accident, the use of nuclear energy remains a need for many countries. Research and development and international cooperation are keys to an optimal development of nuclear energy for the future.

Further reading:

1. *C. Poinssot, B. Boullis, "Actinide recycling within closed fuel cycles," Nuclear Engineering International, January 2012.*
2. *C. Poinssot, D. Warin, C. Rostaing and M. Masson, "Enhancing the sustainability of nuclear energy by increasing the efficiency of actinide recycling processes: overview of the major guidelines," ICCAP 2011 Conference, Nice, France, May 2011.*

The Intriguing High-temperature Studies of Plutonium Dioxide and Mixed Oxide Solid Solutions

This article was contributed by Rudy J. M. Konings and Dario Manara of the European Commission, Joint Research Centre, Institute for Transuranium Elements (JCR-ITU), and by Christine Guéneau of the French Alternative Energies and Atomic Energy Commission (CEA).

The oxides of the transuranic elements have been the subject of numerous investigations since the discovery of neptunium (Np) and plutonium (Pu) in 1940–1941. Similar to uranium oxides, they are stable under atmospheric conditions and do not require complicated synthesis. Once they were produced in substantial quantities they became available for experiments. Early research included their structural, magnetic, and thermodynamic characterization, mainly at ambient and cryogenic temperatures. Only in the 1960s were systematic studies undertaken on the (very) high-temperature properties of the oxides of the transuranic elements. This was in part because the uranium-plutonium mixed dioxide was becoming the prevailing fuel choice for fast reactors, and because the well-studied metal fuel exhibited dimensional instability during irradiation for which solutions were not easily found. Oxide fuel operates at a much higher temperature, only a few hundreds of kelvins below melting, resulting in an almost complete fission gas release, and, hence, a remarkable stability up to high burnup. Moreover, it undergoes a restructuring early in its life, caused by the migration of pores to the center of the fuel under the influence of vapor-assisted mass transport along the temperature gradient (Fig. 1).

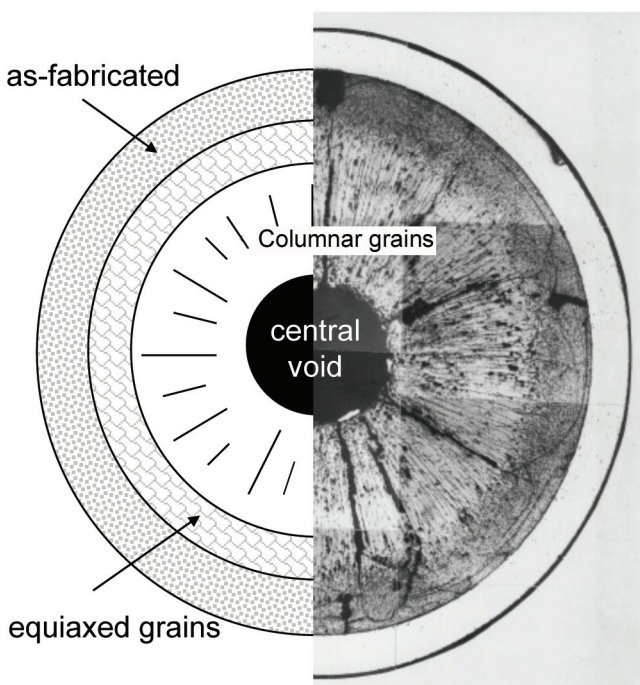

Figure 1. Fast reactor oxide fuel restructuring at high temperature, showing on the right side a photograph of the restructured fuel, and on the left a schematic presentation of the four distinct zones that are formed. Note that the outer ring on the photograph represents the fuel cladding.

The high-temperature studies needed to understand the processes in fast reactor oxide fuel and to determine the safety margins were undertaken in a few laboratories in the US and Europe where these highly radioactive materials can be handled and where very-high-temperature measurement equipment was developed. Melting temperatures were generally determined by thermal analysis of samples encapsulated in refractory metals such as tantalum and tungsten, which were heated in a resistance or induction furnace, a technique widely used in those days. However, the limits of this technique had to be explored because the melting points of the actinide oxides are higher than most other refractory oxides. Also, vaporization studies are far from straightforward, as the behavior of the actinide oxides is complicated by the presence of the AnO_3, AnO_2, and AnO molecules in the vapor, and possibly also with atomic An. To detect these species in substantial quantities, temperatures well above 2000 K are required. Many of the early vaporization studies were made by collection techniques capable of determining the total mass of material vaporized (total pressure), but not the molecular composition (partial pressure). The latter can be determined by using Knudsen cell effusion mass spectrometry, a high-temperature technique that was popular in the 1960s, but the few measurements on the actinide oxides that were made with this technique were not conclusive.

Together with the relatively abrupt end of the fast reactor programs in the 1980s, these high-temperature studies came to a halt. Subsequently, the results available for the actinide oxides have been evaluated by numerous authors. Good agreement existed among these evaluations. For example, for the melting temperature of plutonium dioxide, a value around 2673 K (2400 ^{o}C) can be found in most handbooks based on the works from the 1960s. Doubts about this value were only raised recently in a study on the UO_2-PuO_2 phase diagram by Japanese researchers[1], who reported significant deviations of more than a hundred degrees for the melting temperature of PuO_2, depending on the nature (tungsten, rhenium) and shape of the containments.

It should be stressed that these high-temperature studies of the actinide oxides face two (related) challenges. First, the samples undergo compositional changes upon heating; in particular changes in the oxygen-to-metal ratio caused by formation of oxygen gas and the concomitant partial change in the valence of the metal, and also in the Pu/(U+Pu) ratio because of incongruent vaporization. For example, stoichiometric PuO_2 will transform to $(Pu^{4+}Pu^{3+})O_{2-x}$ and the released oxygen gas can react with its environment. Second, the samples can easily react at the high temperatures of the measurements, particularly when they are molten and the liquid contacts the containment. Innovative approaches are needed to avoid this. In the Japanese work, the solution was sought in alternative encapsulation techniques using more inert materials such as rhenium. In our work at the Institute for Transuranium Elements (ITU), performed in close collaboration with the French Alternative Energies and Atomic Energy Commission (CEA), in the frame of the F-BRIDGE project in the EU Seventh Framework Programme, we have followed different routes.

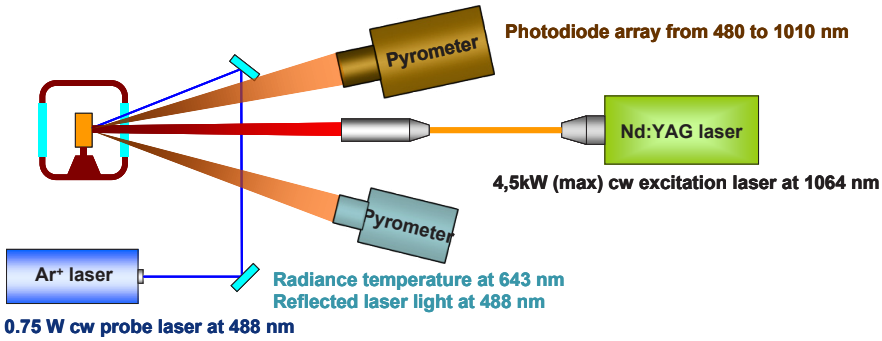

Figure 2. A schematic drawing of the laser melting setup showing the laser beam hitting the sample in the autoclave and the optical analytical tools to measure the temperature, the emissivity, and the state of the surface.

For the melting studies we have explored the potential of a fast laser heating technique developed in-house[2] that creates self-crucible conditions as a result of the liquid always remaining in contact with the solid it is formed from, as explained in Fig. 2. By also controlling the atmosphere during the measurements (air or oxygen), the melting temperature of the virtually stoichiometric composition can be determined. For PuO_2 the experiments resulted in a value more than 300 K higher than the earlier reported values, 3017 K ± 17 K vs 2673 K,[3] a more-than-substantial difference. A slightly smaller difference was found for NpO_2 and its melting temperature, 3070 K ± 62 K, nicely fits in between PuO_2 and UO_2 (3130 K ± 20 K).[4] This leads to a new view on the trend of the melting temperatures of the actinide dioxides—as the nearly linear decrease from ThO_2 to PuO_2 suggested by the earlier results no longer applies (Fig. 3). We feel the newly established trend more closely reflects the gradual changes in the interactions of *f*- and *d*-electron states in the light actinides.

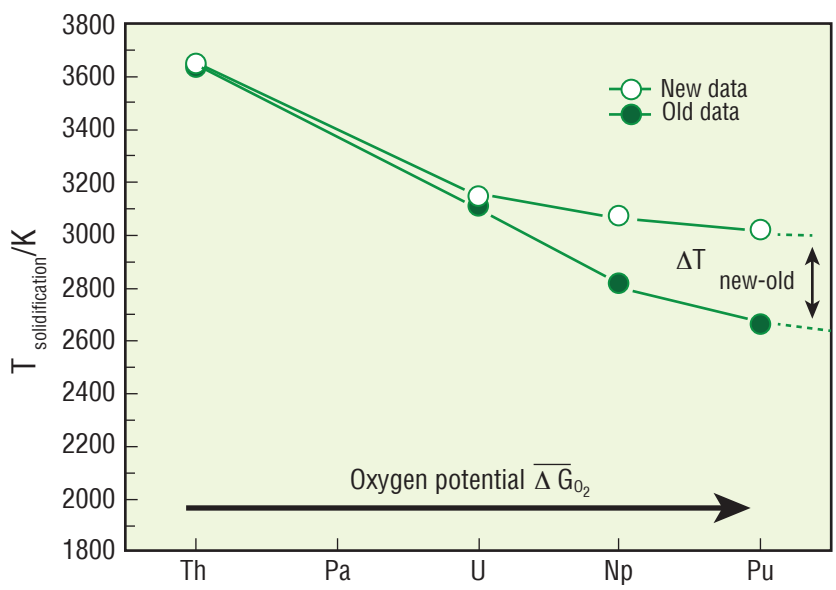

Figure 3. The trend in the melting temperature of the actinide dioxides.

For the vaporization studies we explored a different approach. For example, for the study of the Pu-O system, we have tried to control the composition of the sample in situ in the Knudsen cell of the mass

spectrometer.[5] By adding a flow of oxygen gas (100 Pa) into the cell, the composition of the solid phase can be kept close to stoichiometric, O/Pu = 2, during the measurements. The measurements required a cell made from ThO_2, the only refractory oxide that does not react with the sample. Alternatively, by reacting PuO_2 with plutonium metal, a sample in the two-phase domain (Pu_2O_3+$PuO_{1.6}$) could be studied. For these two experiments, plus one for the congruent vaporization composition for which the composition of the solid and gas phase are identical, the vapor pressure and speciation were determined. For the stoichiometric composition, the vapor consisted almost entirely of molecular PuO_2, but the total pressure in the oxygen flow experiment was found to be higher than that in vacuum. This contradicts earlier assumptions that the PuO_2(cr) = PuO_2(g) equilibrium can be analyzed from measurements in vacuum, and indeed a different enthalpy of sublimation has been derived from our work. A similar experiment for NpO_2 did not reveal this difference between oxygen and vacuum, indicating the stronger bonding of oxygen in this compound. In the case of uranium dioxide, gaseous UO_3 is dominant, however, this species has not been observed for Np or Pu. The vapor above the (Pu^2O_3+$PuO_{1.6}$) two-phase domain was found to be principally composed of molecular PuO with a small fraction of elemental Pu. At the congruent vaporization composition (Pu/O = 1.83 at 2100 K) both molecular PuO_2 and PuO were found to be present.

These results clearly imply the need for revisiting the UO_2-PuO_2 binary phase diagram with the same techniques. The results for PuO_2-rich samples indicated a slight decrease of the melting temperature with decreasing PuO_2 content, which is different than that reported in the literature; the results for the UO_2-rich samples were in good agreement with existing measurements. Thus a new representation of this essential system in nuclear technology was obtained from phase diagram optimization using the CALPHAD approach, as shown in Fig. 4.[6] Vaporization studies in the UO_2-PuO_2 binary system were also performed, but these are very complicated because of changes in O/(U+Pu) and Pu/(U+Pu) ratios. Experiments in oxygen could not be performed because of the risk of

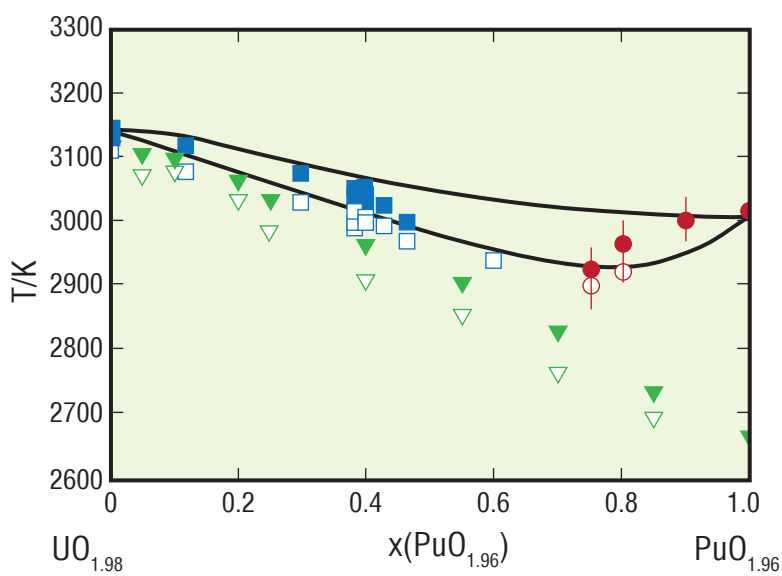

Figure 4. The UO_2-PuO_2 phase diagram. The red symbols represent the new results from JRC-ITU; the other colored symbols show older results. They are projected on the calculated phase diagram $UO_{1.98}$-$PuO_{1.96}$ pseudobinary phase diagram; the end members represent the congruent melting compositions according to the thermodynamic model.

oxidation of uranium. Therefore we have explored the congruent vaporization composition for samples with 25 mol%, 50 mol%, and 75 mol% PuO_2 and checked the consistency of the results with those obtained from combining the thermodynamic model for the condensed phases with the assessed thermodynamic data for the gaseous phases. As is shown in Fig. 5, the overall agreement is very good considering the uncertainties in the experiments and model. Consequently, this agreement holds for the major molecular species but not for the minor vapor species (UO, Pu).

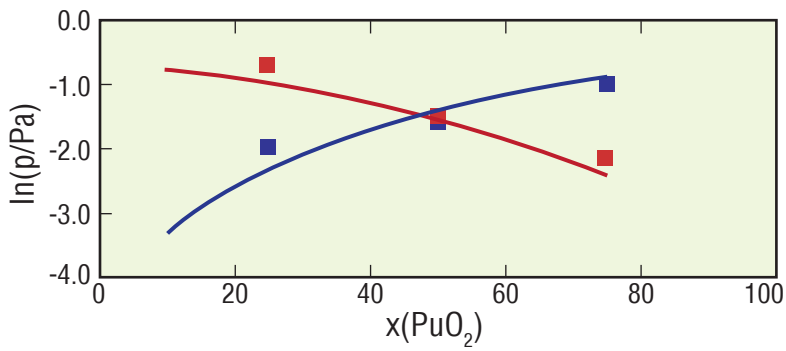

Figure 5. The vapor pressure of plutonium- and uranium-bearing species as a function of Pu composition in the $(U,Pu)O_{2-x}$ samples, in the quasicongruent condition (O/M)s = (O/M)g. The lines show the results of the thermochemical model; the symbols the results from mass spectrometric measurements.

At first sight it is remarkable that such significant errors in essential properties such as the melting temperature have been revealed for the actinide oxides, but retrospectively it can be understood. The decreasing metal-oxygen bond energy going from Th to Pu progressively affects the high-temperature behavior, increasing the equilibrium oxygen pressure to very high values and significantly changing the composition of the solid phases. Although this effect is less prominent at the lowest temperatures in the mass spectrometric measurements, and better agreement with existing studies has been found, it should be taken into account. Our work has shown that with well-planned experiments and supporting modeling, the complex high-temperature behavior of the actinide oxides can be studied successfully. For the U-Pu-O ternary system we have now a fairly reliable understanding. A major challenge will be to extend this system with americium, an important issue for fuels of the next-generation fast reactors for which transmutation capabilities are foreseen.

Further reading:

1. *M. Kato, T. Tamura, K. Konashi, S. Aono, "Oxygen potentials of plutonium and uranium mixed oxide," J. Nucl. Mater. 344 (2005) 235.*
2. *D. Manara, M. Sheindlin, W. Heinz, C. Ronchi, "New techniques for high-temperature melting measurements in volatile refractory materials via laser surface heating," Rev. Sci. Instr. 79 (2008) 113901.*
3. *F. De Bruycker, K. Boboridis, D. Manara, P. Pöml, M. Rini, R.J.M. Konings, "Reassessing the melting temperature of PuO2," Materials Today 13(11) (2010) 52.*
4. *R. Böhler, M.J. Welland, F. De Bruycker, K. Boboridis, "Revisiting the melting temperature of NpO2 and the challenges associated with high temperature actinide compound measurements," J. Appl. Phys. 111 (2012) 113501.*
5. *P. Gotcu-Freis, J.-Y. Colle, J.-P. Hiernaut, R.J.M. Konings, "(Solid + gas) equilibrium studies for neptunium dioxide," J. Chem. Thermodyn. 43 (2011) 1164.*
6. *C. Guéneau, N. Dupin, B. Sundman, C. Martial, J.-C. Dumas, S. Gossé, S. Chatain, F. De Bruycker, D. Manara, R.J.M. Konings, "Thermodynamic modelling of advanced oxide and carbide nuclear fuels: Description of the U–Pu–O–C systems," J. Nucl. Mater. 419 (2011) 145.*

This article was contributed by John R. Beddington, Graham A. Fairhall, and Francis R. Livens. John Beddington is the UK Government Chief Scientific Adviser and chaired the Nuclear Research and Development (R&D) Advisory Board, that carried out the 2012 review of UK nuclear R&D. Graham Fairhall is Chief Science and Technology Officer of the UK National Nuclear Laboratory (NNL), and Francis Livens is Research Director of the University of Manchester's Dalton Nuclear Institute. Both Fairhall and Livens contributed extensively to the work of the R&D Advisory Board.

A New Focus for the United Kingdom's Civilian Nuclear Research and Development

Background

It seems fitting that, in the year 2012 when the United Kingdom (UK) hosted the Plutonium Futures conference, its government moved to re-evaluate the future role of nuclear energy in the UK energy supply, and the need for R&D to underpin this future role, including production of a nuclear R&D roadmap to 2050.

The UK has a long history of civilian nuclear power, stretching back to the 1950s, when the Magnox reactors, the first commercial power reactors in the world, were introduced, and the UK has operated a closed fuel cycle for over half a century. More recently, though, the industry's story has been one of decline, with the last UK reactor start-up in 1995 and a contraction of the civilian nuclear R&D base over the years that followed.

The year 2002 represented a major turning point for the UK, as the government recognized the need to deal with the accumulated nuclear legacy and, through the creation of the Nuclear Decommissioning Authority (NDA) in 2005, reoriented the industry to a decommissioning and cleanup mission. The NDA has a £100 billion (about $150 billion) work program, expected to last over a century. High hazard, historic waste facilities are being emptied and dismantled, reactors have been shut down, defueled, and are being left 'cold and dark' prior to final decommissioning, and there is a clear process leading towards geological disposal of higher activity wastes (Intermediate Level Waste, vitrified High Level Waste, and unreprocessed spent fuel). As we have seen recently in West Cumbria, UK, the geological disposal program is based on identification of a volunteer host community and establishment of a community/government partnership to implement geological disposal.

Reflecting the rundown in the nuclear industry, the UK's nuclear energy production has now fallen from a peak demand of about 25% in the late 1990s to 11 GWe (about 19% of demand today). However, the government has started to address the implications of its ambitious carbon reduction targets (to 20% of 1990 levels by 2050), and it has become clear that nuclear energy will probably play a greater future role in the UK energy supply mix. The first step is to move towards new nuclear construction, and the government foresees up to 16 GWe of light water reactor (LWR) construction by 2025–2030, operating an open fuel cycle and providing about 20% of electricity production. The decision to proceed with the first of these new reactors is expected early in 2013. Beyond these immediate plans, many UK energy scenarios on a 40- to 50-year timescale imply a substantial further increase in nuclear energy production in the range of 40 to 75 GWe, including the option to operate a closed fuel cycle.

It is in this context that the UK government has set up an ad hoc Nuclear R&D Advisory Board (NRDAB) in early 2012, with wide-ranging terms of reference (Fig. 1). Here, we summarize key elements of the Board's work.

The UK's Nuclear R&D Landscape

As part of its work, the R&D Advisory Board carried out a study of the current R&D landscape in the UK, that provided some unexpected results. The UK is sometimes seen as a nation that *used to do* nuclear R&D; in fact, it still does a considerable amount, with approximately 40% of the effort being devoted to fusion R&D and 60% to fission. Annual government spending on nuclear R&D is approximately £66 M (about $100 M), divided evenly between fission and fusion. In addition, the NDA supports around £120 M (about $180 M) per year of R&D in its mission areas (decommissioning, waste management, and geological disposal), mostly at high technology readiness levels. Further R&D is funded by industry mainly to support ongoing reactor operations and through participation in international programs, particularly European R&D. The total fission R&D expenditure is difficult to estimate, but is probably around £180 M (about $270 M) per year.

The UK civil nuclear fission R&D community is currently staffed at over 1,200 strong, spread across industry, national laboratories, and academia, and there are also over 400 fission-focused Ph.D. students in the UK.

This level of activity is substantially lower than 30 or 40 years ago (the R&D community is about 20% of the size it was in 1980, while funding is only at 7% of the 1980 level). However, the UK still retains significant expertise across the nuclear fuel cycle, developed in many cases from the national R&D programs in the 1980s and 90s, and this is nevertheless a significant foundation on which to build. In particular, there is substantial expertise in high-temperature materials from the Advanced Gas Cooled Reactor fleet, and in recycling from many decades of operating a closed fuel cycle. More recently, there has been a substantial expansion in decommissioning capability due to the NDA's program.

Regenerating Skills

However, there are substantial challenges to this R&D community, with many of the R&D leaders being far closer to the end of their careers than the beginning. Over half of this community will retire within 10 years and, given the time needed to develop world-class R&D leaders, there is an immediate need to take action to ensure continuity. The proposal is that all stakeholders (industry, academia, regulators, and the national laboratories) work together to create a clearly defined R&D career path, removing obstacles and uncertainties so that the next generation can assume R&D leadership as soon as possible. This will be coupled with active transfer of expertise from retired and retiring experts to the younger generation through a Senior Fellowship program to facilitate effective mentoring. A key requirement for the success of this initiative will be the implementation of longer term R&D programs enabling scientists and engineers to gain experience, including working in international collaborations.

R&D To Meet Future Needs

The UK's current R&D effort is very focused on specific topics, reflecting a combination of commercial drivers and government priorities over the past decade, with the majority being directed towards support for the currently operating reactor fleet, or the NDA decommissioning and waste management programs (Fig. 1). Given the implications of government's Carbon Plan for the UK's future nuclear energy program, the UK needs to invest now in an R&D capability (skills, facilities, and programs) to support development and deployment of advanced reactor systems and their associated fuel cycles. Expanded R&D in this area will also allow the UK to play a more active role in relevant international collaborations such as the Generation IV International Forum and European programs. In addition, as the UK looks further into the future and starts to consider new and unproven technologies, there is a need to be able to evaluate these to make an objective and rational analysis of fuel cycle alternatives 'from cradle to grave,' and understand the technical, financial, political, social, safety, and security implications of our choices. Developing a methodology for doing this is an early R&D priority.

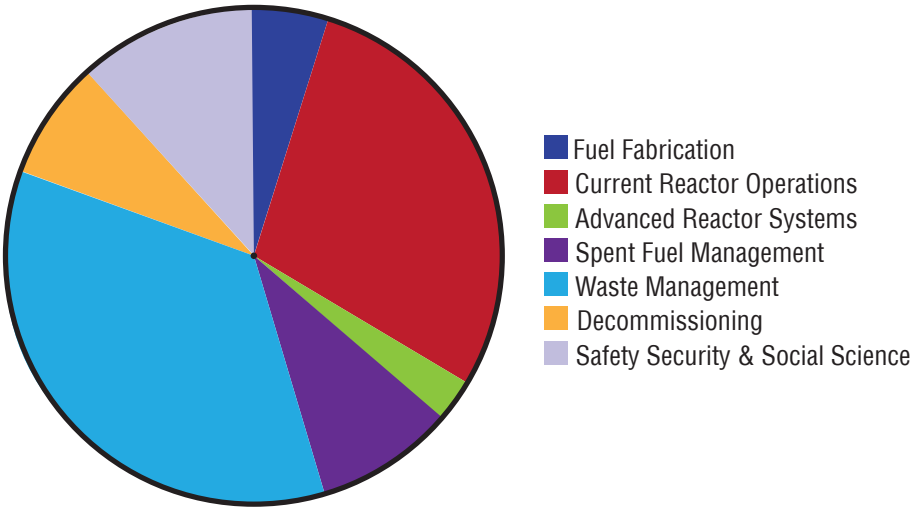

Figure 1. UK nuclear R&D effort by program area.

R&D Facilities

Nuclear R&D requires specialized facilities, and while the UK has in the past had a wide range of facilities, including experimental fuel manufacturing and post-irradiation examination facilities, active pilot plants for fuel cycle studies and prototype reactors, these have largely been lost over the last 20–30 years. However, the National Nuclear Laboratory (NNL), created in 2008 during the restructuring of British Nuclear Fuels Limited, inherited some newly built state-of-the-art active nuclear R&D facilities (Fig. 2), including plutonium gloveboxes and hot cell facilities. Since its creation, NNL has been working to commission, equip, and open these facilities to the wider research community, as one of three core facilities of a "National Nuclear User Facility" (NNUF) in which the other facilities are the Culham Centre for Fusion Energy and The University of Manchester's Dalton Cumbrian Facility, which supports decommissioning engineering R&D and experimental radiation science.

Coordination of Nuclear R&D

It became clear during the Board's work that the present arrangements to sponsor and manage UK nuclear R&D are very complex, involving many different actors, both national and international, and each with their own assignments and agendas. Consequently, there is a need to improve coordination of nuclear R&D activities within government, with support from and involvement of the wider R&D community.

Concluding Remarks

The UK's nuclear R&D needs are changing rapidly as civilian nuclear fission regains importance in the future energy supply mix. The current focus on support for the UK's current reactor fleet, and on the NDA's decommissioning and cleanup programs, reflects previous priorities and needs to be supplemented with R&D to support future nuclear generation and fuel cycles. In all areas, the development of next-generation, high-level R&D skills represents a major challenge, which requires rapid, coordinated action. These changes to a much more forward-looking R&D program are likely to transform the UK nuclear landscape over the next few years. Papers from the Nuclear R&D Advisory Board have been published by the government beginning in the spring of 2013.

Further Reading

The UK Government's Carbon Plan (The Carbon Plan: Delivering Our Low Carbon Future) and associated documents are available online.

Figure 2. Central laboratory R&D facilities operated by NNL.

This article was contributed by Georgios Koutroulakis of Los Alamos National Laboratory and Hiroshi Yasuoka of the Advanced Science Research Center, Japan Atomic Energy Agency.

First Observation of ^{239}Pu Nuclear Magnetic Resonance

Plutonium is arguably one of the most complex elements of the periodic table. It exhibits a multiplicity of oxidation states and a pervasive tendency to form a range of nonstoichiometric phases in the solid state. As a consequence, it also remains the most enigmatic among the heavily used elements. Nevertheless, it has become enormously important since it was first synthesized in the early 1940s. With plutonium being ubiquitously present at the core of nuclear arsenals and one of the cornerstones for the world's energy production, the understanding of its fundamental properties and behavior is of utmost interest. Thus, any experimental technique that can potentially provide useful information about this perplexing element, and the plethora of its compounds and molecules, constitutes a rather valuable tool.

Nuclear magnetic resonance (NMR) has evolved into one of the most widely used techniques for the study and characterization of materials at the atomic and molecular level. NMR has revolutionized the practice of chemistry, physics, and medicine by providing a noninvasive method for probing and imaging matter on a microscopic scale. Moreover, it is being used in numerous technological applications in a variety of fields.

The NMR technique is based on the fact that most nuclei behave like small magnetic dipoles due to their quantum mechanical property of possessing a finite spin angular momentum I. For this reason, when found in the presence of an external magnetic field, a nucleus interacts with it through the so-called Zeeman interaction. This interaction leads to a well-defined number of allowed energy configurations for the nucleus. Specifically, we get 2I+1 equally spaced energy levels with $E=-\gamma_n \hbar I_z B_0$, where B_0 is the magnetic field applied parallel to the z-axis, I_z is the spin component along the z-axis, $\hbar$ is Planck's constant h divided by 2π, and γ_n is the nuclear gyromagnetic ratio. If the exact amount of energy corresponding to the difference between two adjacent levels can be delivered to the system, a resonance occurs when transitions between these levels are induced. In an NMR experiment, this energy ΔE is provided to the nucleus by an appropriate electromagnetic pulse of frequency f_n, so that the resonance condition is simply $2\pi f_n=\gamma_n B_0$ (Eq.1). From the latter equation, it is evident that the gyromagnetic ratio γ_n effectively constitutes the fingerprint of a specific nucleus.

In real materials, the nuclei of the atoms are not isolated since they interact with their surrounding electrons, as well as with one another. The effect of these interactions can be thought of as an additional, internal magnetic field that the nuclei sense. It is through the investigation of this very effect that NMR can provide a window to the material's electronic properties in a rapid and nondestructive way. In other words, the nuclei serve as 'spies'

of their electronic environment. A characteristic, well-known example of the utility of NMR in complex systems is that of magnetic resonance imaging (MRI), which is nothing but NMR performed on the body's protons, i.e., the nuclei of hydrogen atoms, in order to recreate an image of soft tissues.

Among the approximately 30 nuclear isotopes of the periodic table featuring a nuclear spin of I=1/2, ^{239}Pu is the only one that has yet to be observed by NMR, in spite of more than 50 years of effort on a range of compounds. There are two primary reasons why ^{239}Pu NMR has remained elusive for so long. First, the value of the gyromagnetic ratio g_n, the defining characteristic of a nucleus in terms of NMR as explained earlier, is not accurately known. In fact, the relevant theoretical predictions vary wildly. Consequently, from a quick look at Eq. 1, it is apparent that we do not know around which frequency to search for the NMR signal for a given applied field value. Second, and more important, the unpaired electrons in the Pu atom couple to the spin of its nucleus very strongly, resulting in an extremely strong internal magnetic field at the nuclear site. This in turn can shift the resonance frequency by orders of magnitude, and also forces the nuclei to relax back to their equilibrium state after the resonance pulse so quickly that any NMR measurement is practically impossible.

The way we went about circumventing the latter challenge, that of the excessively strong electron-nuclear spin interaction, was to attempt NMR measurements on a very pure sample of PuO_2. In PuO_2, when the sample is cooled to low temperature (for our experiments, 4 kelvins, or -452.47 ºF, -269.15 ºC), the Pu^{4+} ions are in a nearly nonmagnetic state. For this reason, we anticipated the interaction to be somewhat minimized so that an NMR signal could be observable. As for the problem of not knowing the value of the gyromagnetic ratio γ_n, we just swept a really wide range of external magnetic fields for a given frequency value, hoping to "hit" the value that would satisfy the resonance condition of Eq. 1.

Our first successful experimental run (Fig. 1) comprised standard pulsed NMR technique measurements with the sample at a temperature of 4 K, where the pulse frequency was kept constant at f=16.51 MHz, and the external magnetic field was varied between 3T (Tesla) and 8T. An obvious signal was seen for B_0=5.8T. *This is the first observation of a ^{239}Pu NMR signal.* Detailed measurements followed, where we carefully traced the pairs of frequency-field values that satisfied the resonance condition (see Eq.1). From there, we constructed the relevant f-B_0 plot. This procedure is illustrated in Fig. 2. Then, the value of γ_n in PuO_2 is simply given by the slope of this graph, as can easily be seen from Eq.1. This value is derived from a linear fit to the data to be $^{239}\gamma_n(PuO_2)/2\pi$ = 2.856 ± 0.001 MHz/T. Of course, the bare gyromagnetic ratio, i.e., that of an isolated ^{239}Pu nucleus, will be different from the one we deduced from our experiments in PuO_2, since, as discussed above, in the latter case there is an internal magnetic field contribution arising from the various interactions in the material. Hence, after correcting for this contribution, we estimate the bare γ_n value of the ^{239}Pu nucleus to be $^{239}\gamma_n/2p \approx 2.29$ MHz/T.

Figure 1. Georgios Koutroulakis and Hiroshi Yasuoka in the condensed-matter NMR lab at Los Alamos National Laboratory after having observed the magnetic resonance signal of ^{239}Pu for the first time.

Similar experiments were also conducted on a second PuO_2 sample known to be not as pure; that is to say, containing significant amount of impurities. The goal was to ascertain the validity of our results for the pure sample by comparing them to those found when a slightly altered electronic environment is sensed by the nuclei. As expected, the measured NMR spectrum in this case was apparently different, attesting that the detected NMR signal is really associated with the material's Pu nuclei.

Considering the utility of NMR in other areas of the periodic table, our finding of the ^{239}Pu NMR signal in PuO_2 could open new frontiers for the physics and chemistry of actinide compounds. This would provide, first of all, a long-awaited proof of concept, and, importantly, a guide of where to "look" by specifying the gyromagnetic ratio of the ^{239}Pu nucleus. It invites further studies in a range of materials and under a range of conditions in various branches of actinide science. Especially in view of the technological importance of plutonium compounds for nuclear fuels, power generation for interplanetary exploration, and long-term storage of nuclear waste, the ability to probe local structure and electronic environment of the nucleus by ^{239}Pu NMR should prove particularly powerful.

This research was partially funded by the Glenn T. Seaborg Institute and the Los Alamos National Laboratory Directed Research and Development program. Support was also provided by the Chemical Sciences, Geosciences, and Biosciences Divisions and by the Materials Sciences and Engineering Division, Office of Basic Energy Sciences, U.S. Department of Energy (DOE). High-purity plutonium oxide was provided by the Surveillance and Monitoring Program at LANL supported by DOE Nuclear Materials Disposition EM-3.

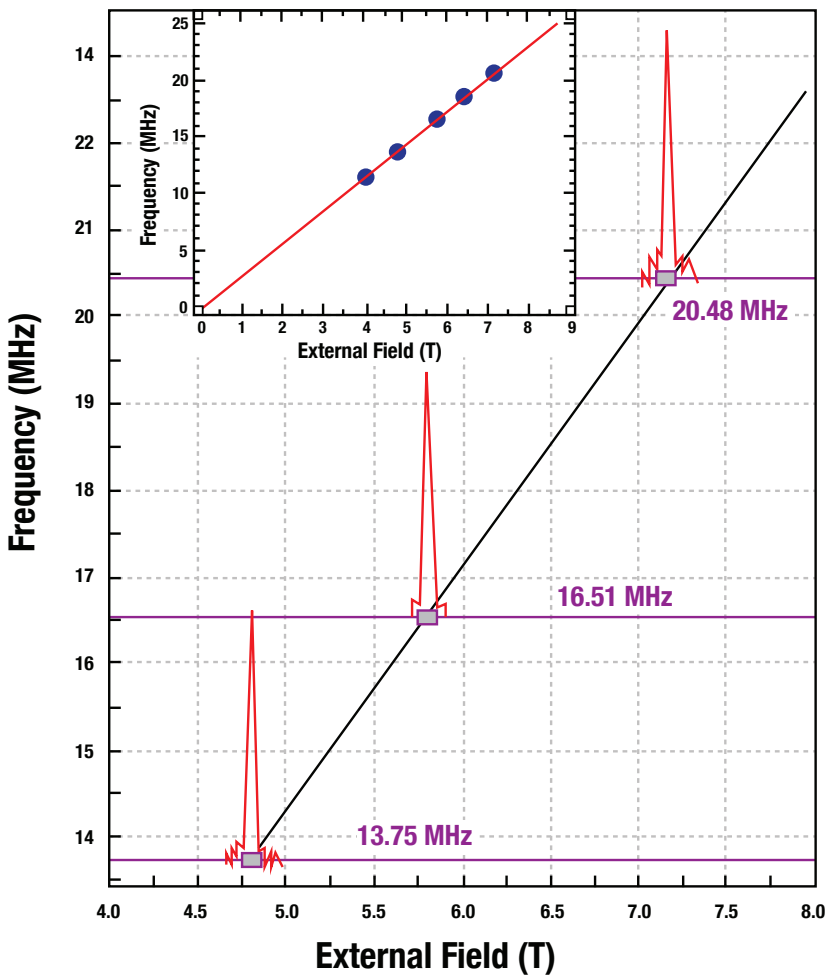

Figure 2. ^{239}Pu NMR spectra in PuO_2 recorded at different pulse frequencies. Using the values of the f-B0 pairs for which the signal is detected, the plot of the inset is sketched. The relevant slope gives us the gyromagnetic ratio of the Pu nucleus in PuO_2, whose value is $239\gamma_n(PuO_2)/2\pi = 2.856 \pm 0.001$ MHz/T.

Further reading:

H. Yasuoka, G. Koutroulakis, H. Chudo, S. Richmond, D. K. Veirs, A. I. Smith, E. D. Bauer, J. D. Thompson, G. D. Jarvinen, D. L. Clark, "Observation of ^{239}Pu Nuclear Magnetic Resonance," Science 18 May 2012: Vol. 336, no. 6083 pp. 901-904.

This article was contributed by Paul Cook of Sellafield Ltd and by Howard Sims and David Woodhead of the United Kingdom National Nuclear Laboratory.

Safe and Secure Storage of Plutonium Dioxide in the United Kingdom

Reprocessing operations at the Sellafield site in Cumbria, United Kingdom (UK), have resulted in the production of a large amount of PuO_2 (Fig. 1). While some of this material has been reused, the majority remains on the Sellafield site pending decisions on its final disposition. The operators of the Sellafield site are required to ensure this material is stored in a safe and secure manner, potentially for many decades; the timescale for storage now being longer than was originally anticipated. When considering the design of PuO_2 storage systems, the following three key requirements need to be addressed:

- Containment must be maintained at all times, including fault scenarios. Two barriers are required. Packaging is generally one layer and the second layer is storage.
- Security of the material must be maintained at all times. PuO_2 held at Sellafield is subject to safeguards requirements.
- Storage of the PuO_2 product must preserve options for reuse. This dictates that it must not become contaminated or experience temperatures that drive changes to the physical properties of the powder.

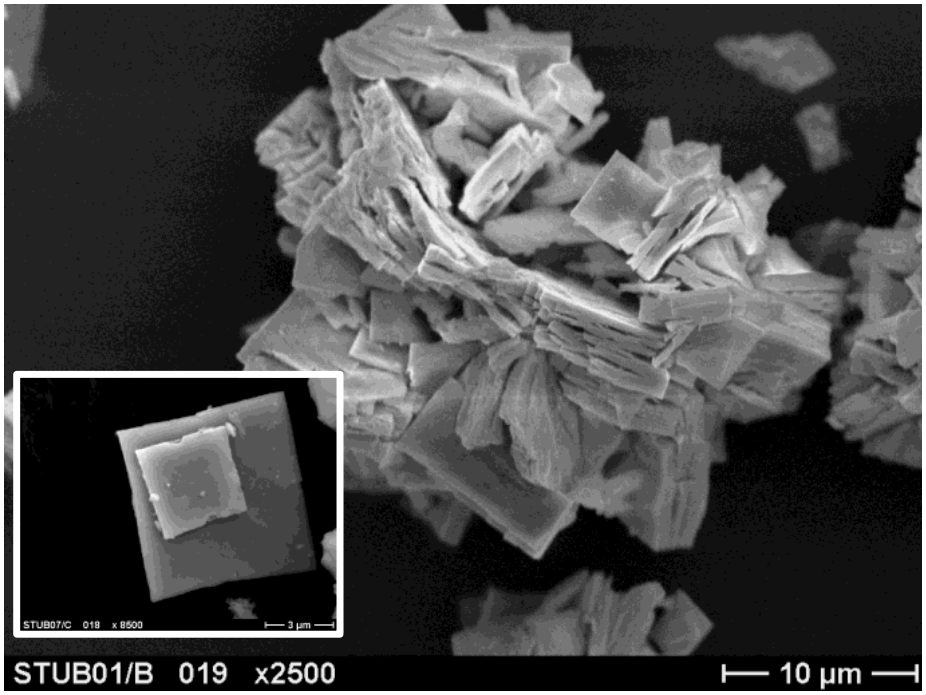

Figure 1. A scanning electron microscope image of a PuO_2 particle produced by oxalate precipitation at Sellafield. The image shows the high surface area of the particle relative to its overall volume.

Figure 2. The Thorp 3-can arrangement. Bar codes are present on each can for identification purposes.

To provide containment and prevent contamination of the product, all PuO_2 produced since the mid-1970s has been packaged in welded containers. Two designs are used: Magnox PuO_2 product is held in a screw-top aluminium inner can and a welded stainless steel outer can with an intermediate polyethylene bag. The Thermal Oxide Reprocessing Plant (Thorp) product is held in a stainless steel 3-can system (Fig. 2), with some similarities to the DOE-3013 design. A potential problem with welded cans is the possibility of pressurization. This may have many causes, including the following:

- Gas law pressurization due to self-heating
- Helium in-growth as a result of alpha decay
- Gas generation from degradation of polythene intermediate layer in Magnox packages
- Desorption of adsorbed gases (notably steam)
- Radiolysis of moisture

The first two mechanisms apply in all cans. While they can be quantified there is limited scope for controlling them. An outstanding question and subject of ongoing research is the extent to which helium is released from the powder matrix. Practical experience of can storage shows

that this is less than 100%, although there is limited evidence that in the longer term release fractions increase.

Radiolytic and thermal degradation of polythene have been studied extensively. Results demonstrate that in anaerobic conditions and typical dose rates polythene is relatively robust, and high temperatures are needed to drive degradation. Magnox cans are stored in the cooler storage areas to further limit the potential for polythene degradation.

The final two mechanisms can be managed by control of the product quality; both surface area (SSA) and retained moisture, along with thermal conditions in the storage area.

To limit the potential for pressurization, a series of requirements, known as CFAs (conditions for acceptance) are placed on cans before they are accepted into storage. To specify appropriate CFAs, the following interlinked factors should be considered:

- Temperature distribution through the package and its contents. The thermal behavior of the whole storage area needs to be understood as well as that of individual packages (Fig. 3).
- Behavior of moisture in response to the temperature profile. Models have been developed to describe the relationship between temperature, atmosphere above the powder, and surface water concentration. In high-moisture cans water will redistribute as the can self-heats.
- Radiolysis and how it is affected by local conditions in the powder.

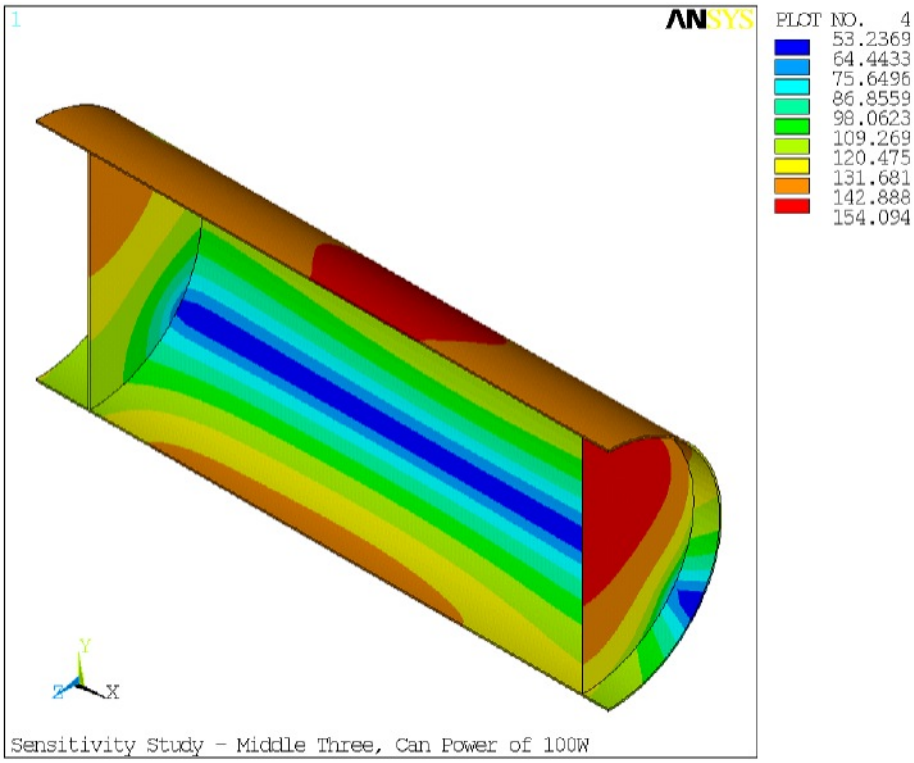

Figure 3. The predicted temperature distribution around the outer can of a 100-W Thorp package is shown. The coolest region around the can 4 o'clock position corresponds to contact with the support rails.

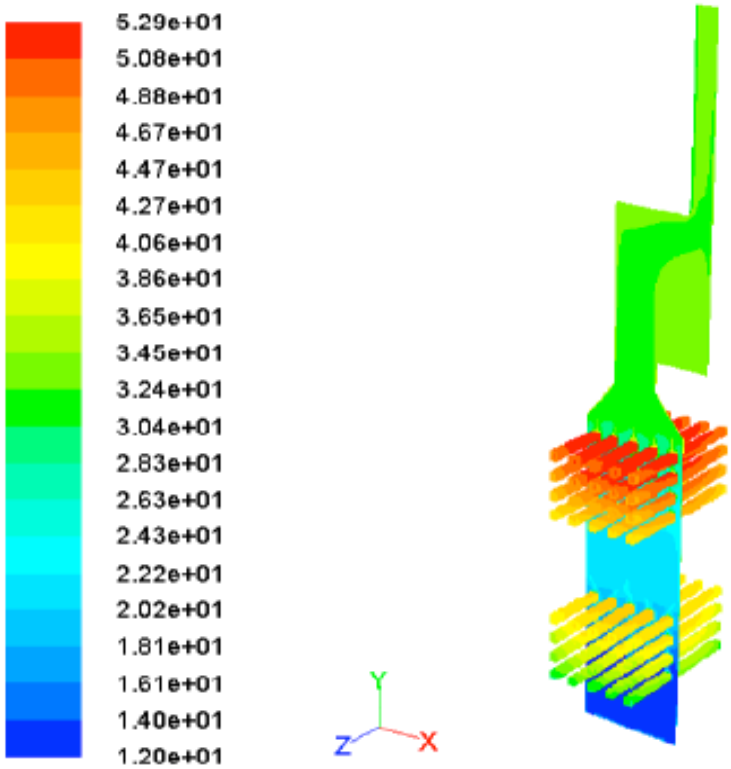

Figure 4. The predicted temperature distribution for a storage cell in SPRS from the CFD model. The temperature is shown in °C, and incoming air is assumed to be at 12 °C.

Work in all these areas has been undertaken by the National Nuclear Laboratory (NNL) and Sellafield Ltd in recent years. The methods described are applied to all product storage but have been further refined during commissioning of the Sellafield Product and Residues Store (SPRS), which has recently been completed.

SPRS is a naturally cooled storage facility where the airflow is provided by buoyancy effects from the decay heat inside the cans and is the first of its type in the UK. Prior to operation it was shown that under a range of operational and bounding conditions temperatures could not rise to the level where significant can pressurization occurs. For proof, two models were created (Figs. 3 and 4). A detailed finite element thermal model was built to provide definition of temperatures inside individual cans. A computational fluid dynamics (CFD) model was developed to determine the local air temperature around the cans based on the overall heat load within the building and external factors, such as incoming air temperature.

During commissioning of the storage facility it was necessary to show that the predictions of these models were cautious so that a margin of safety was demonstrated. Over 150 measurements of can-surface temperatures were obtained along with continuous monitoring of air temperatures and flows inside the building. Overall it was shown that the models provide a good basis for predicting can temperatures, but a number of notable results were obtained. In particular, the temperature distribution around a storage can is complex and there are qualitative differences in the results from Thorp (3-can) and Magnox (2-can) packages. At the storage level, the impact of wind on air flows can be significant; this has been considered in safety case scenarios.

Desorption of moisture from the surface of PuO_2 is currently estimated from the work of Stakebake and, more recently, Paffett. More work is being undertaken to better characterize adsorption/desorption relationships for Sellafield-produced material, and results from this will be incorporated in models when they become available. Knowing how temperatures vary through the powder and understanding the adsorption/desorption behavior has led to the development of process models that describe the distribution of water through the can as well as predicting the partial pressures of the various gaseous species present. It is then necessary to determine whether there is a radiolysis hazard arising as a consequence of the predicted water distribution within the powder.

Radiolysis of water on the surface of PuO_2 would be expected to form hydrogen. On many oxides, including CeO_2 and UO_2, this gives very high yields of H_2 (G_{H_2} significantly greater than for bulk water) in the first few monolayers because of energy transfer from oxide to water. However this does not appear to occur with PuO_2, which displays the opposite trend: G_{H_2} is significantly less than bulk water in the first few monolayers and increases with monolayer coverage. Work has been carried out at the NNL to measure the hydrogen yield from Magnox- and Thorp-derived material with results shown in Fig. 5. The graph requires SSA data, which is not always available, so this has been estimated from data on decomposition of oxalate found in literature. Data are presented as G_{H_2} in water by taking into account dose partition in the two phases according to stopping powers of $^4He^{2+}$. Limited water uptake measurements on PuO_2 have been carried out that show that at high SSA and high RH water uptake may be limited compared with lower SSA PuO_2. Reasons for the different radiolysis behavior of PuO_2 are not known. It is possible that energy transfer does not occur in highly radiation-damaged solids or that the products of energy transfer to water react at the surface. Similarly the surface would be expected to be reactive towards oxidizing and reducing radicals that may interfere with the primary processes forming H_2.

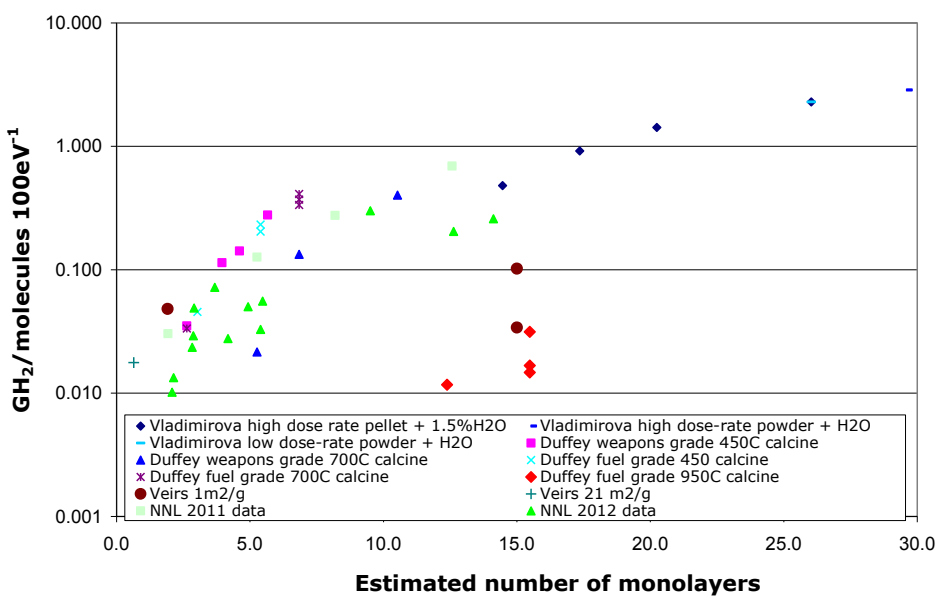

Figure 5. Plotting formation of G_{H_2} for a variety of stored nuclear materials and (estimated) monolayers.

Figure 5 shows that H_2 should still be formed slowly at low water coverage, but since only a few cans with very high water content have pressurized, a thermal or radiolytic recombination reaction must occur on the PuO_2, the nature of which is currently under investigation.

Using knowledge of can temperatures and understanding the pressurization mechanisms, it is possible to predict can pressures for a range of inputs. Working backwards, it is then possible to place limits on absorbed moisture and power to define the CFAs. This process has proven to be successful at Sellafield with less than 0.05% of the can population experiencing any difficulties during storage. This process can also be used as a tool to identify those cans that may benefit from further surveillance. A capability for in-situ monitoring of storage cans has been developed to increase understanding of conditions. Taken together, these actions will help to ensure the safe and secure storage of the material for many decades to come.

Future research planned includes developing an understanding of water uptake and its dependence on SSA, radiolysis on the surface of PuO_2, recombination reactions, and helium release. We will study helium release by puncturing real cans in a new purpose-built laboratory.

Plutonium Futures
The Science 2012

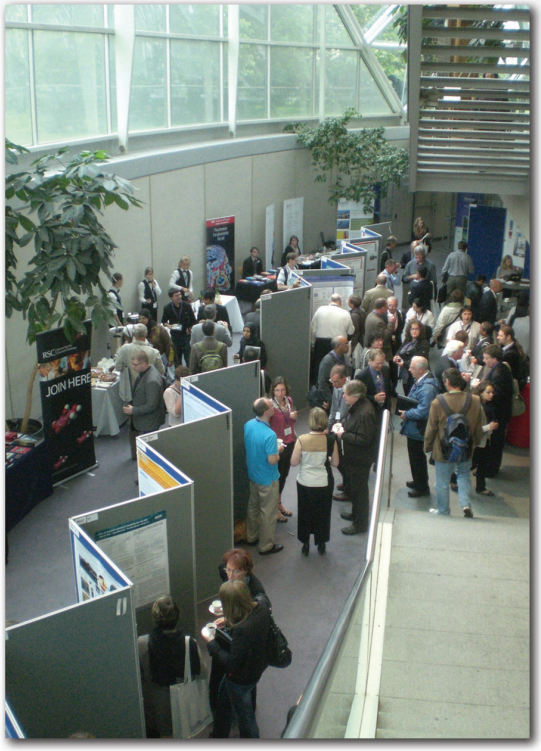
JOIN HERE

Prof. Sir Mark Welland FRS FREng
Director of the Nanoscience Centre,
University of Cambridge
Monday, 16 July 2012
IOP Institute of Physics
Plutonium Futures
The Science 2012
15 – 20 July 2012,
University of Cambridge, UK
www.PuFutures2012.co.uk

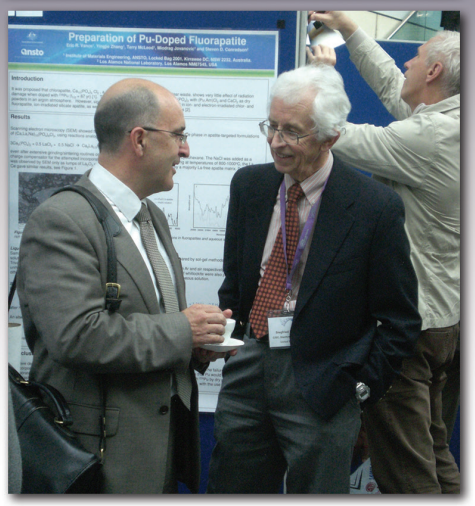

Plutonium Futures
The Science 2012

Cambridge, United Kingdom,
from July 15–20

Photo captions: see page 51

This article was contributed by Boris A. Nadykto of the Russian Federal Nuclear Center, VNIIEF Sarov, Russia.

Alpha Decay in Plutonium, Radiogenic Helium, and Plutonium Swelling

The α-decay yielding ~5 MeV α-particles (^{4}He nuclei) and recoil nuclei, ~85–90 keV isotopes of uranium, is the primary decay channel for Pu. The decay heat is important because in order to avoid damage of materials undergoing or exposed to the radioactive decay a natural or artificial heat absorber is required. The lifetime and decay heat rate of Pu are known to vary from isotope to isotope. For example, the decay heat of ^{239}Pu with the half-life of 24,000 yr is about 2 W kg^{-1}. Much lower decay rate and decay heat rates are observed in the case of Pu-242 and Pu-244 given their much longer half-lives (3.75 x 10<5> and 8.08 x 10<7> yr, respectively).

The impact of the decay products on materials exposed to the radioactive decay was noted almost immediately after the discovery of the α-decay. In 1907 Irish geophysicist John Joly explained the appearance of "pleochroic halos," colored spherical shells of ~10–30 μm radius, in natural crystals resulting from an impact of α-rays emitted from microscopic inclusions of uranium-containing minerals. Two perfectly logical questions: "Why α-particles do not damage the crystal structure along the entire pass?," and "How do low-energy and slow α-particles at the end of their journey become so dangerous?" can be answered after we compare the electronic structures of α-particle He^{2+} and He atoms. Compact α-particles He^{2+}, which are He nuclei, lose their energy in collisions with electrons of the host material and cannot damage the crystal lattice due to the very small collision cross section with host material nuclei. In contrast, α-particles at the end of their pass, which instantaneously grow ~10^3 times bigger via $He^{2+} + 2\,e^- \rightarrow He$ reaction, are capable of damaging the crystalline lattice. The collisions of the electronic shells of He atoms and atoms of the host material lead to the displacement of the host material atoms from the equilibrium position and damage of the crystalline structure. Of course, the radioactive decay in natural minerals is typically slow and, hence, making damage to the crystalline lattice visible may take millions or perhaps hundreds of millions of years.

Damage to the crystalline lattice of metallic Pu is usually caused by the recoil atoms located ~10 nm from the decay point. Uranium-containing inclusions, which are ~100 million years old, may produce similar defects in natural minerals due to the recoil nuclei (Th) formed via the uranium decay inside the inclusions in which the number of decay events (~2% of total number of U nuclei) is close to what would occur in 500-yr-old ^{239}Pu oxide. Such defects could not be traced back in 1907; however, impressive progress has been made in state-of-the-art experimental techniques over the last century, which now makes their discovery possible.

The formation of bubbles filled with inert gases inside the macroscopic samples of radioactive metals affected by large radiation doses is a very important problem for actinide sciences. These phenomena frequently occur in nuclear reactors and are usually explained by the high mobility of atoms of nuclear materials at high temperatures. According to the conventional theory, the He bubble formation in metallic Pu occurs via clustering of point defects followed by growth of bubbles, or pores, being formed. The diffusion of the surrounding Pu atoms leads to the migration of vacancies and clusters of vacancies filled with He, which is followed by their association as larger pores and bubbles via the coalescence. All the point defects, their clusters, pores, and bubbles move inside the metallic Pu due to the thermal motion of the surrounding atoms. The migration of He bubbles and pores in metallic Pu occurs via the transport of atoms of the host material (Pu) from the frontal side of a bubble or pore to the opposite side. The main transport mechanisms include the diffusion of Pu atoms alongside the bubble surface (M1), volume diffusion of Pu atoms in the immediate vicinity of the bubble (M2), and the diffusion of evaporated Pu atoms inside the bubble (M3). Typically, M1 dominates at temperatures of (0.3–0.5)T_m. In this case, the pressure inside bubbles and total volume of bubbles remain constant after the coalescence due to the low mobility of the vacancies. In the case when the bubble radius is below 1 nm and, therefore, the He density inside the bubble is very high, the surface diffusion, M1, gets suppressed and the volume diffusion, M2, becomes the dominant diffusion mechanism (Fig.1).

The equilibrium condition for the gas bubble is given by the well-known expression $P-2\gamma/R+\sigma-\sigma'=0$, where *P* is pressure inside the bubble, $2\gamma/R=P_L$ is the Laplace capillary pressure, σ is the internal stress in the host material, and σ' is the external stress in the host material. The surface tension of Pu γ is ~0.55 N m^{-1} near the melting point. Being largely controlled by the interatomic forces, γ for Pu depends on temperature only weakly. When the bubble radius is small (~0.7–1.0 nm), PL=1.6-1.1GPa, respectively. Therefore, ^{4}He inside the bubble can no longer be considered an ideal gas. In this case, an equation of state accounting for the real gas properties should be applied.

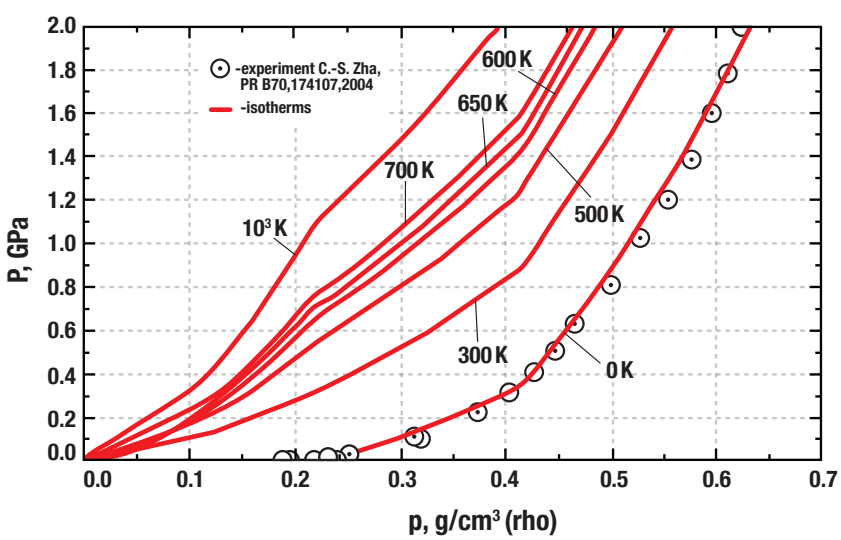

Figure 1. Equation of state for ^{4}He. Experimental data are adopted from Zha, Mao and Hemley.[2]

When the capillary forces are not strong enough to balance the gas pressure inside the bubble, equilibrium can be achieved due to the influence of the shear stress and viscosity of the host material. In this case, He pressure inside the bubble P-2γ/R+GB/R, where *G* is the shear modulus of Pu and *B* is the Burgers vector, can be higher than the equilibrium Laplace pressure P_L=2γ/R. The elevated pressure in large bubbles may appear due to the uptake of a large number of small bubbles, in which the He pressure is very high due to the capillarity/Kelvin effect. Here it is important to note that one can not expect bubbles to be spherical due to considerable shear stress impacts.

The density of He inside nanosized bubbles can be determined by measuring the shift of the $1s^2\ {}^1S_0$-$1s2p\ {}^1P_1$ transition line in He under hydrostatic pressure using the electron energy loss spectroscopy (EELS). The EELS measurements indicate a substantial growth of the pressure beyond the capillarity limit (Laplace pressure) in He-implanted Al up to the saturation of the sample by He ranging from 3 to 26 at. %.[5] The bubble radius was found to be in the range of 0.65–2 nm. The pressure inside the bubbles was ~5.5–13 GPa that is ~4–5 times higher than the Laplace pressure. The bubble growth typically begins after the yield strength point is achieved. The bubble growth below the yield strength point may occur via diffusion creep—the uptake of the neighboring vacancies.

Figure 2 shows micrographs from the transmission electron microscopy (TEM) study of Jeffries et al.,[4] but many studies have been undertaken. Zocco and Rohr investigated the 10-yr-old δ-phase Pu-Ga alloys after annealing at 400 °C revealed the presence of nano-sized 7.3 nm and 10–17 nm diameter bubbles filled with He.[16] More recently, Schwartz et al. (2001, 2003, 2005) observed in their transmission electron microscopy (TEM) study the formation of helium bubbles in the δ-phase Pu-Ga alloy aged from 16 to 42 yrs at room temperature. The average bubble radius (~0.7 nm) and bubble number concentration (<1.5×10^{17} cm^{-3}) for Pu aged from 19 to 42 yrs were found to depend on the Pu age only weakly. It was proposed that the small He bubbles are formed due to migration and

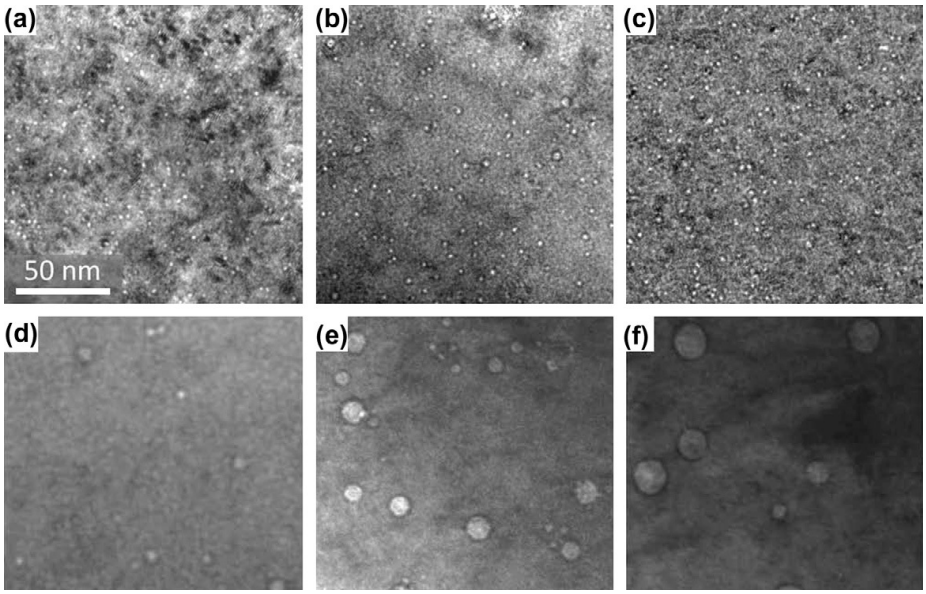

Figure 2. Bright-field TEM micrographs of He bubbles in naturally aged and annealed Pu-Ga specimens. Each micrograph is of a 160×160 nm area. Note that the scale bar is included only in (a). The He bubbles are seen as white, circular objects within the darker, gray matrix of the Pu-Ga specimen. The individual panes correspond to specimens undergoing the following annealing treatments: (a) naturally aged, (b) 325 °C for 2 hr, (c) 325 °C for 24 hr 375 °C for 90 hr, 425 °C for 2 hr, 425 °C for 24 hr.[4]

coalescence of vacancies filled with He, which are formed as Pu is aging. More details on the discovery of He bubbles in Pu at room temperature can be found in Issue 4 of the *Actinide Research Quarterly* (2001).

Jeffries et al. have studied the growth of helium bubbles due to the migration and coalescence in thin samples of Pu-Ga alloys. The annealing temperatures and times were ranging from 250 °C to 425 °C, and 2 to 90 hrs, respectively. The investigation of naturally aged samples has also been carried out. The samples, whose age was typically ~42 yrs, were studied using TEM at room temperature after annealing (Fig. 2).

Annealing temperature, time (age)	Mean diameter (nm)	P_L, GPa, (ρ, g/cm^3)	Number density of bubbles, (10^{17}/cm^3)	Number of He atoms, (10^{19}/cm^3)	Number of He atoms in bubbles, (10^{19}/cm^3)	He fraction in bubbles	Volume fraction of bubbles (%)
Nat. aged/42y	1.4	1.57 (0.51)	0.94	6.9	1.0	0.15	0.014
250°C/2h/42y	1.3	1.69 (0.47)	1.99	6.9	1.6	0.23	0.023
250°C/24h/42y	1.3	1.69 (0.47)	1.13	6.9	0.9	0.13	0.013
325°C/2h/42y	1.4	1.57 (0.43)	1.42	6.9	1.3	0.19	0.02
325°C/24h/42y	1.4	1.57 (0.43)	0.9	6.9	0.8	0.12	0.013
375°C/90h/20y	5.2	0.42 (0.16)	0.074	3.3	1.3	0.40	0.054
425°C/2h/42y	7.9	0.28 (0.12)	0.121	6.9	5.6	0.81	0.31
425°C/24h/42y	10.9	0.20 (0.08)	0.073	6.9	5.9	0.86	0.49

Table 1. Properties of He bubbles in Pu-3.3 at. % Ga alloys. Alloy age is 42 or 20 yrs.[4]

Table 1 shows measured parameters of helium bubbles as well as the pressure P-2γ/R and density of He inside the bubbles at pressure *P*, that was estimated based on the equation of state for real matter.[4] Based on the data from Table 1, one can calculate, using the bubble density and bubble number concentrations, the amount of He in the bubbles and its ratio to the total amount of He accumulated in the sample due to the α-decay.

The calculations show that the ratio at T<325 °C does not exceed ~0.2 in agreement with the estimates based on the experimental data of Schwartz et al. at room temperature.[14] However, at T = 425 °C, the ratio increases to ~0.8. This probably indicates that the diffusion flow of He to the bubbles is growing as the temperature increases. However, it is also possible that a marked increase in pressure and density of He inside the bubbles of ~1 nm in radius appears due to the influence of the Pu strength. It is possible when the strength of small domains of Pu surrounding bubbles is close to the theoretical strength limit. It is important to note that the strength of the macroscopic/bulk Pu is much lower and cannot affect the bubble pressure and density of He. At 300 K–600 K, the pressure inside the bubble P-2γ/R + GB/R (G=6–12 GPa and B=0.3 nm for d-phase Pu) is ~4–5 times higher than the capillary/Laplace pressure. Under such conditions the total amount of He in bubbles can grow by a factor ~2, reaching the level of 40% of the total amount of He accumulated in the sample. At T=425 °C nearly all the

helium is located in bubbles under the capillary pressure. This means that in the case of 4–5 nm bubbles the strength properties of the bubble walls are close to those of bulk Pu. At T=450 °C the coalescence of two bubbles of close size due to migration and collision in Pu-Ga alloy was observed by Jeffries et al. No Oswald ripening, the gradual change in the bubble size due to the He diffusion, was found. The experiments of Jeffries et al. lead us to the following conclusions:

- No change in the bubble diameter after annealing at T≤325 °C for 2 hr and 24 hr was observed. This means that both the diffusional growth and migration and coalescence are probably suppressed due to the low mobility of Pu atoms.
- Annealing for 24 hrs at T= 250 °C and 325 °C leads to a marked decrease in the bubble number concentration compared with the 2-hr annealing. The most probable cause of the observed decrease is the escape of the bubbles from the sample due to the extremely small sample thickness.
- The bubble coarsening, which begins at T= 375 °C after 90-hr annealing, is observed at T= 425 °C after 2-hr annealing. The bubble diameters (~5–10 nm) at these temperatures are consistent with those obtained in the earlier study of Zocco and Rohr.

However, the bubble diameters measured by Jeffries et al. at T = 425 °C deviate by ~3 orders of magnitude from those found by Wheeler and Bayer[15], who under similar conditions (temperature and annealing time) have observed ~700 nm bubbles using an optical microscope.

Wheeler and Bayer show that at high temperature the annealing of 31-yr-old Pu-Ga alloy is a two-stage process (Fig. 3). At the first stage, the samples shrink due to the annealing of defects. The first stage is followed by stage two leading to the He bubble growth and sample expansion. The He bubble size distribution observed in their study is "quasi-bimodal," largely consisting of submicron (~700 nm) and "breakaway" bubbles of several tens of microns.

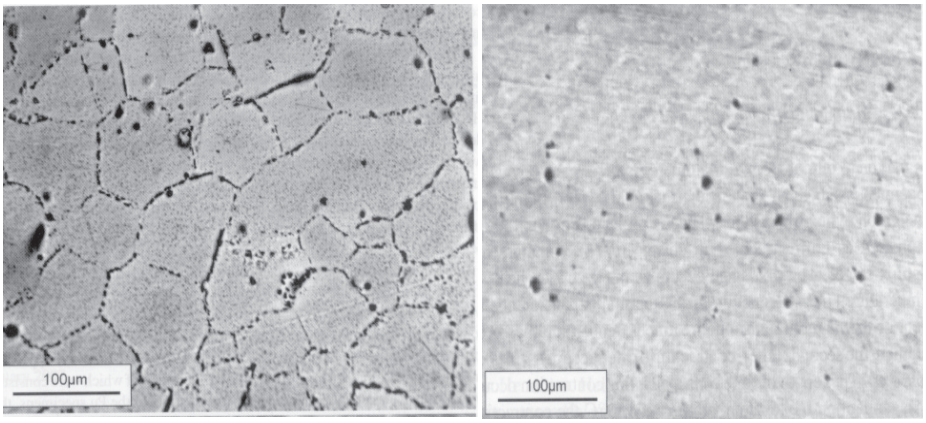

Figure 3. Optical micrographs of 31-yr-old Pu-3.4 at. % Ga heated to 300 °C for 306 hr in the etched (left) and unetched (right) states.[15]

Table 2 shows measured parameters of helium bubbles[15] as well as pressure P=2γ/R and density of He inside the bubbles at pressure *P* estimated based on the equation of state for the ideal gas. Wheeler and Bayer found a marked swelling of Pu at 400 °C, which may be related to the observed

helium bubbles of micron size containing small amount of He (1%–2%) after the 16-hr annealing. However, annealing for 336 hrs leads to the growth by an order of magnitude in both the He concentration in the bubbles and bubble volume. Time needed in order to reach the same bubble size was found to decrease dramatically with increasing temperature. The "breakaway" bubbles also contain small fractions of He. According to Wheeler and Bayer, after annealing for 16 hrs at *T*=400 °C large "breakaway" bubbles were not observed. After 336-hr annealing the amount of He in breakaway bubbles was an order of magnitude lower than that in smaller submicron bubbles. The fraction of total volume of 30–60 μm bubbles after 3-hr annealing at T=600 °C was found to be a few percent. The experimental data show that thermal desorption of He from solid Pu heating to the melting point does not exceed 10% of the accumulated helium; that is close to the amount of He contained in the breakaway bubbles.

Annealing temperature/ time	Mean diameter (μm)	P_L, bar (ρ , 10^{-4} g cm^{-3})	Number density, cm^{-3}	Number of He atoms in bubbles, 10^{18} cm^3	Fraction of He in bubbles	Volume fraction of bubbles (%)	Number "breakaway" bubbles of He, 10^{18} cm^3	Volume fraction of breakaway bubbles (%)
200 °C/188 h	–	–	–	–	–	–	1.4	2.8
300 °C/306 h	0.5	44 (39)	7.1×10^{10}	2.7	0.0541	0.5	0.3	0. 6
400 °C/16 h	0.7	31 (24)	5.6×10^{9}	0.36	0.007	0.1	–	–
400 °C/363 h	0.8	27 (21)	5.3×10^{10}	4.5	0.088	1.4	0.4	0.8
500 °C/16 h	28	0.78 (0.53)	8.8×10^{6}	0.8	0.016	10	–	–
500 °C/336 h	60	0.37 (0.25)	8.8×10^{6}	3.7	0.072	100	–	–
600 °C/3 h	30	0.73 (0.44)	7×10^{6}	0.64	0.013	9.8	0.97	1.9

Table 2. Bubble diameter and other bubble properties in 31-yr-old Pu-3.3 at.% Ga alloys.[15]

Since at temperatures of 400–500 °C the experimental shear modulus of the Pu-Ga alloy is ~8–10 GPa, one can expect its value at 600 °C to be about 6 GPa. At temperatures above 500 °C, the equilibrium He pressure in bubbles of >30 μm in radius is below the atmospheric pressure. The estimates of $P=2\gamma/R + GB/R$ inside 60–90 μm breakaway bubbles yield the pressure range of 1–0.6 atmospheres. It is possible that melting can lead to a marked decrease in the total volume occupied by large breakaway bubbles accompanied by the simultaneous growth of the smaller submicron bubbles due to the enhanced mobility of Pu atoms. The helium release from a melting sample depends on the sample dimensions, bubble size, and temperature due to the strong dependence on temperature of the Pu viscosity.

These considerations lead us to conclude that the controversies over the recent Jeffries et al. and Wheeler and Bayer studies can be easily resolved. Our analysis suggests that most of He in the Pu-Ga alloy at 400 °C in Jeffries' study is located inside ~10 nm diameter bubbles, that were observed in the TEM and were invisible in the optical microscope used by Wheeler and Bayer. On the other hand, the bubbles of 700–1000 nm diameter cannot be observed in the TEM studies of samples of 40-nm thickness and surface area of 160×160 nm.

Although the controversies over the recent Jeffries et al. and Wheeler and Bayer studies are largely resolved, the mechanism or mechanisms responsible for the bubble formation at room temperatures remain poorly understood. The association/coalescence of point defects and their clusters is doubtful due to the very slow diffusion at such temperatures. Unfortunately, no experimental data on the diffusion coefficient for Pu-Ga alloys at low temperatures are available at the present time. The experimental diffusion coefficient grows by a factor of 10^3 as the temperature is growing from 600 K to 800 K. The extrapolation of the experimental data to the room temperature of 298.15 K gives us the value of 10^{-28} , which is lower than that at 600 K by a factor of 10^{15}. Another important detail is that Jeffries et al. showed that the bubble growth beginning at T=375 °C occurs at T=450 °C solely due to the bubble migration and coalescence with no diffusion of He from smaller to larger bubbles.

A model of the formation of primary defects due to the recoil atoms that is based on the consideration of shock-wave impacts of the recoil atoms on the surrounding media, was developed by B. Nadykto and O. B. Nadykto.[10] In the framework of this model, moving uranium atoms are considered as spheres of bulk U. The speed of the U atoms decreases with the path length due to momentum transfer from U atoms to surrounding Pu atoms, leading to the decrease of the pressure behind the shock front. The model points out the possibility of the formation of nano-sized defects/pores without nucleation, solely due to the influence of recoil atoms. The evaporation of the host material behind the shock front occurs when the thermal energy is higher than the heat of vaporization. In this case, the host material density quickly decreases due to the high thermal pressure. The following quick cooling leads to the formation of free volume.

Another possibility for the rapid formation of the initial free volume in alloyed δ-Pu is related to the well-known $\delta \rightarrow \alpha'$ phase transformation under high hydrostatic pressure.[3] This transformation leads to a 25% increase in the Pu density and can create free volume of ~2 nm radius due to the recoil atoms. The free volume may, however, be reduced due to the rapid cooling and inverse $\alpha' \rightarrow \delta$ transformation. The recoil atoms induce melting of Pu within the volume of ~10 nm in radius because of the rapid heat transfer due to the thermal conductivity. On the other hand, cooling leads to the recrystallization of Pu in the same volume. The recrystallization volume is close to the volume of the host material containing a single bubble of 1.4 nm in diameter at low temperatures. Every new decay event closes all the bubbles contained in the 10-nm domain and forms a single bubble 1.4 nm in diameter. This means that the number of bubbles in 40-yr-old Pu is 300–600 times fewer than that of α-decay events. The recrystallization volume contains at 0–300 °C about 300–600 He atoms, a 20%–40% fraction of which can fill the free volume during relaxation after the decay. A perfectly logical question: "Where are the remaining He atoms going?" is yet to be answered. However, it is possible that they exist in the form of vacancies containing one or two He atoms.

In order to gain new insights into the nature of the nano-bubble formation in Pu, the density of He inside the nano-sized bubbles should be measured. Such an experimental study can be carried out using EELS method

based on the measurements of the shift of $1s^2\ ^1S_0$-$1s2p\ ^1P_1$ transition line in He under compression. The application of the EELS is well justified because the bubble size distribution at room temperature is narrow and that increases the accuracy of the EELS measurements. The equation connecting the shift of the $1s^2\ ^1S_0$-$1s2p\ ^1P_1$ transition line in He (ΔE) where the He density is given by $\Delta E = 6.75((\rho/0.169)^{2/3}/2-(\rho/0.169)^{1/3})$, where ΔE is the shift (eV) and ρ is the density (g cm^{-3}). At $\rho \geq 0.5$ g cm^{-3} the linear dependency $\Delta E = 3.27\rho - 1$ can be used.

In order to achieve a clear and insightful understanding of the He bubble formation in metallic Pu the following two questions should be answered: (1) Does the bubble size remain unchanged after aging at very low temperatures of a few tens Kelvin?; and (2) Are the sizes of He bubbles in δ- and α-phases of Pu identical at the room temperature?

Further reading:

1. *R.G. Haire, S. Heathman, M. Idiri, T. Le Bihan, A. Lindbaum, J. Rebizant, "Pressure-induced changes in protactinium metal: Importance to actinide-metal bonding concepts," Phys. Rev. B 67, 134101 (2003).*
2. *C.S. Zha, H. Mao, R.J. Hemley, "Elasticity of dense helium," Phys.Rev. B 70, 174107 (2004).*
3. *S.S. Hecker, D.R. Harbur, T.G. Zocco, "Phase stability and phase transformations in Pu–Ga alloys," Prog. Mater. Sci. 49 (3), 429-485 (2004).*
4. *J.R. Jeffries, M.A. Wall, K.T. Moore, A.J. Schwartz, "He bubble coarsening by migration and coalescence in annealed Pu-Ga alloys," Journal of Nuclear Materials 410, 84-88 (2011).*
5. *W. Jäger, R. Manzke, H. Trinkaus et al., "The density and pressure of helium in bubbles in metals," Radiation Effects Vol. 78, Issue 1-4, 315 (1983).*
6. *Y.K. Vohra, J. Akella, "5f bonding in thorium metal at extreme compressions: Phase transitions to 300 GPa," Phys. Rev. Lett. V. 67. 3563 (1991).*
7. *T. Le Bihan, S. Heathman, M. Idiri, G.H. Lander, "Structural behavior of α-uranium with pressures to 100 GPa, Phys. Rev., B 67, 134102 (2003).*
8. *A. Lindbaum, S. Heathman, K. Litfin, et al., "High-pressure studies of americium metal: Insights into its position in the actinide series," Phys. Rev. B 63, 214101 (2001).*
9. *B.A. Nadykto, "A semi-empirical model for calculating energies of states of multi-electron atoms and ions," Physics-Uspekhi 36(9), 794-827 (1993).*
10. *B.A. Nadykto, O.B. Nadykto, in Ageing Studies and Lifetime Extension of Materials, L.G. Mallinson, Ed., 415-417, 183-189 (2000).*
11. *B.A. Nadykto. Meterialovedenie (Materials Sciences Transactions, in Russian), 5, 2-6 (2005).*
12. *B.A. Nadykto. Instability of the electronic structure of actinides under the high pressure," J. Alloys Compd. 444-445, 241-245 (2007).*
13. *B.A. Nadykto, "Alpha decay in plutonium, radiogenic helium and plutonium swelling," Plutonium Futures–the Science 2012, Cambridge, UK (2012).*
14. *A. Schwartz, M.Wall, T. Zocco, W. Wolfer, Phil. Mag. 85, 479-488 (2005).*
15. *D.W. Wheeler, P.D. Bayer. "Evaluation of nucleation and growth of helium bubbles in aged plutonium," J. Alloys Compd. 444-445, 212 (2007).*
16. *T. Zocco, D. Rohr. Mater. Res. Soc. Symp. Proc. 115, (Specimen Prep. Transm. Electron Microsc. Mater.), 259-264 (1988).*
17. *T. Zocco, A. Schwartz, "A brief history of TEM observations of plutonium and its alloys," JOM, 55(9), 24-27 (2003).*

This article was contributed by J. Somers, I. Farnan, L. Martel, O. Pauvert, C. Selfslag, and T. Fanghänel of the European Commission, Joint Research Centre, Institute for Transuranium Elements.

High-resolution Magic Angle Spinning Solid State

Nuclear Magnetic Resonance Facility for Actinide-bearing Compounds

Solid-state nuclear magnetic resonance (NMR) using magic angle spinning (MAS) is a very powerful analytical method as it is element-specific and sensitive to short-range and atomic-scale structure (Fig.1). Moreover, this technique permits the study of amorphous samples and minor crystalline phases, sometimes beyond the detection limits of X-ray diffraction (XRD). In 2007, Ian Farnan, Herman Cho, and William J. Weber, at Pacific Northwest National Laboratory (PNNL), caused a stir in the actinide community with a MAS-NMR investigation of α-irradiation damage in natural and $^{238/239}$Pu-doped zircons ($ZrSiO_4$).[1] In this pioneering work, they used two levels of containment to house a monolithic ceramic sample.[2] A third barrier against the dispersion of radioactive material was provided by the zirconia rotor (i.e., sample holder) itself.

At the Joint Research Centre's (JRC) Institute for Transuranium Elements (ITU), we were immediately enthusiastic about this breakthrough and sought to establish a similar facility in Europe. Discussions with Herman Cho and Ian Farnan led us to develop their concept further. We wanted to find a concept that would do the following:

- Simplify sample preparation, especially to enable measurement on powders
- Improve the radioprotection against a potential rotor crash
- Push the spectral resolution to the state of the art and reach spinning speeds up to 65 kHz

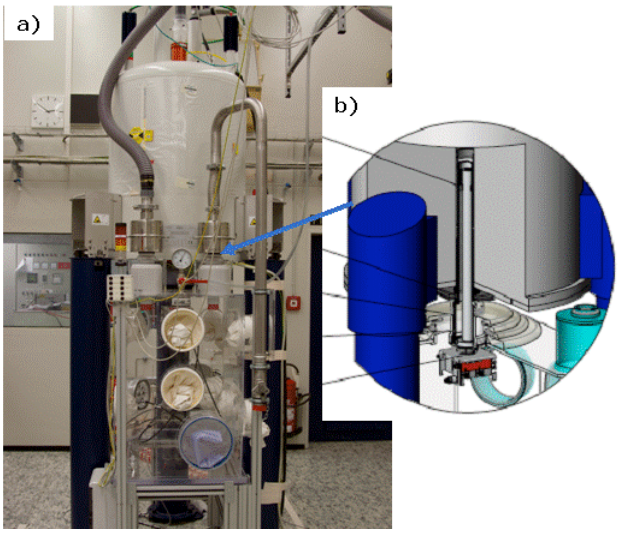

Figure 1. a) The 9.4T Bruker NMR spectrometer and the active glovebox underneath, and b) Schematic representation of the probe located in a Plexiglas tube in the magnet.

While Ian Farnan and Herman Cho decided to isolate the sample with a triple containment rotor, we decided to isolate the entire probe hermetically. The ingenuity of the design lies in an active glovebox that sits on wheels under a wide-bore Bruker 9.4T (400 MHz, ^{1}H frequency) NMR spectrometer, delivered with longer-than-usual support legs.[2] The glove box extends into the magnet core by means of a cylindrical extension made of Plexiglas. A narrow-bore MAS probe with a modified length and tuning connection, which can be accessed using the glovebox glove, is inserted into this tube from inside the box. The MAS probe is housed permanently in the glovebox, and the commercial rotors are loaded there. Thanks to its mobility, the glovebox can be easily removed from under the magnet once the cylindrical extension is pulled back into it. Figure 1 shows the spectrometer and glovebox and a schematic representation of the connections to the glovebox. Control tests on various standards indicate that the glovebox has no effect on the spectrometer performance in terms of signal intensity and resolution.

In the previous experiments of Farnan et al., the rotor speed was limited to 3.5 kHz, mainly due to the need for a large diameter rotor to house the triple containment isolation. This speed was high enough for the study of the ^{29}Si MAS spectra. Nevertheless, strong electron-nucleus coupling between paramagnetic actinides and other nuclei in a material can cause a loss of resolution. Even if the spectrum is broken up into a manifold of spinning side bands this makes site identification difficult.[3] The use of small rotors with very high spinning speeds is the easiest and best solution to overcome the problem. Also, the containment is moved from inside the rotor and the entire probe is isolated. The result of this approach is illustrated in our study of the ^{17}O NMR spectra of (U, Th) mixed dioxide solid solution (Fig. 2). At moderate spinning speeds (15 kHz) ^{17}O NMR spectra of $(U_{0.6}\ Th_{0.4})\ O_2$ exhibit numerous spinning sidebands, but at 55 kHz the spectra are much improved. There is now only a small amount of spectral intensity in

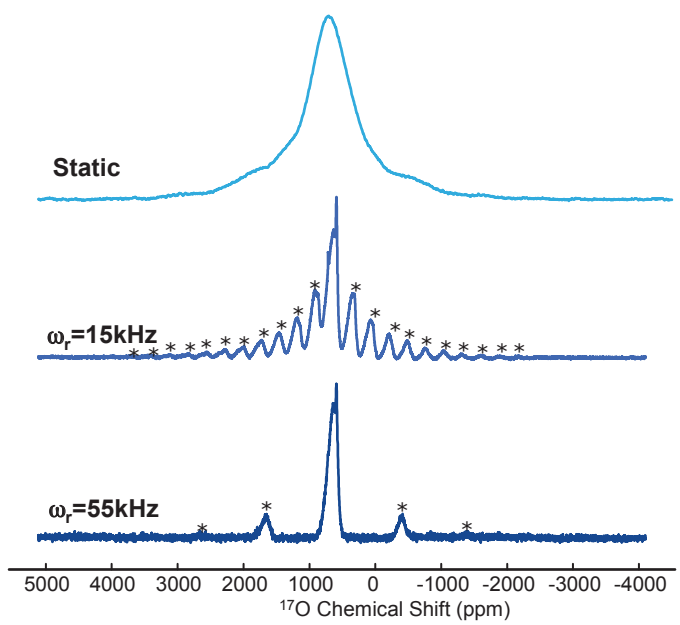

Figure 2. Improvement of the ^{17}O spectral resolution with the MAS frequency for the solid solution $(U_{0.6}Th_{0.4})O_2$ sample. The stars indicate the spinning sidebands.

the spinning sidebands, which are well separated, and there is a substantial increase in the intensity 'spun into' the isotropic peaks. This improves the overall sensitivity of the experiment, allowing oxygen with only Th first neighbors (sharp) and those with U/Th neighbors (broad) to be distinguished and their intensities compared with models for the distribution of U/Th in the structure.

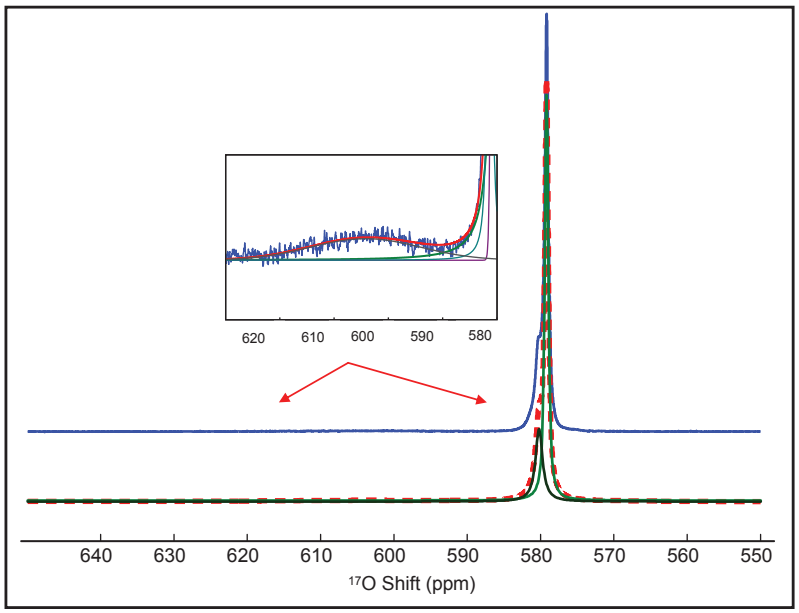

Figure 3. ^{17}O MAS spectrum of $(Th_{0.99},U_{0.01})O_2$ acquired at 55 kHz (top) and its corresponding fit (below) showing peaks due to O surrounded by a distribution of Th and U atoms in the first and second metal shells.

The ^{17}O NMR spectrum from a $(Th_{0.99}U_{0.01})O_2$ sample demonstrates the intriguing possibilities at such high resolution (Fig. 3). The main feature at 579 ppm corresponds to oxygen surrounded by four Th atoms in the fluorite structure (i.e., O-Th_4 subunits). An additional peak at 580 ppm is identified and is due to O atoms surrounded by a first shell made up of four thorium atoms, shifted due to the presence of U atoms in the next metal shell. Closer examination of the data reveals a low intensity feature at 604 ppm due to O surrounded by three Th atoms and one U atom. This sample was prepared by a sol-gel method, and though we were always confident (based on XRD measurements) that this synthesis route yields excellent solid solutions, it was only with this method that the true randomness of the metal atom distribution could be verified.

June 4, 2012 was a memorable day for the JRC-ITU research team with the acquisition of the first ^{17}O MAS-NMR spectrum on PuO_2 at 55 kHz (Fig. 4). The spectral resolution for the ^{17}O peak improves, and the full width at half maximum (FWHM) decreases from 4000 in the static measurement to 400 Hz. The corresponding data for ThO_2 and UO_2 had already been measured in the commissioning phase and those for NpO_2 and AmO_2 since then.

MAS-NMR applied to actinide-bearing compounds is still in its infancy. We have made a number of studies on uranium carbide fuels (^{13}C), sodium uranates (^{23}Na), ^{238}Pu-xenotimes (^{31}P) and irradiated borosilicate glasses (^{29}Si, ^{11}B, ^{27}Al). The outlook is excellent, and much new and exciting information on the local atomic structure in actinide materials is foreseen,

which include the following:

- Identification and quantification of minority phases in fuels
- Investigation of the homogeneity of actinide mixed oxide solid-solutions
- Identification and quantification of irradiation damage in both fuels and glasses and ceramic waste forms

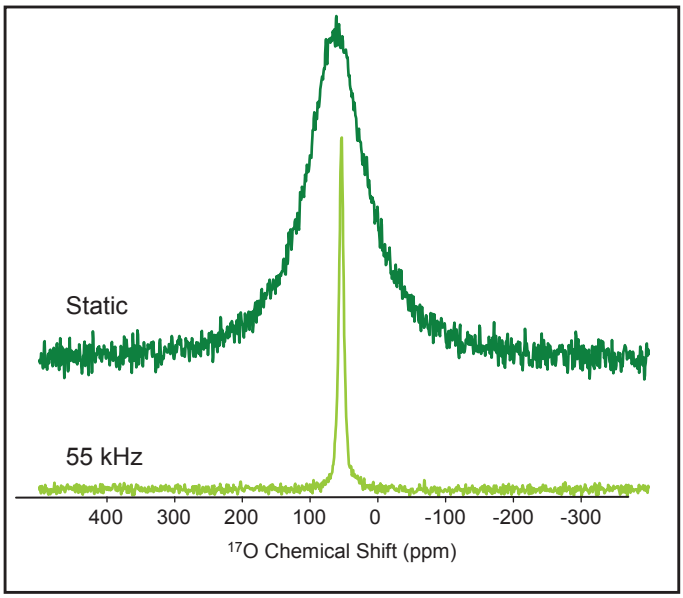

Figure 4. The ^{17}O MAS-NMR spectrum of the PuO_2 sample.

The MAS-NMR developments at PNNL and JRC-ITU mark an important breakthrough, but we also believe that the true potential of NMR will only be achieved when the theory describing these physical phenomena is fully developed and understood for 5*f*-electron systems. Further, efficient combination of NMR with other techniques, in particular extended X-ray absorption fine structure (EXAFS) and XRD, will enable full understanding of the local structure and will provide excellent input data against which ab initio and molecular dynamics codes can be tested and qualified.

Many people have contributed to this development at JRC-ITU, in particular the engineers and technicians who designed and constructed the glove box (Christian Berkmann, Franz Koepp, and Alfred Rothermel). Its realization would not have been possible without the Bruker Corporation instruments; recognizing Bruker staff members Detlef Müller, Stefan Steuernagel, and Christian Steffen.

Further reading

1. *I. Farnan, H. Cho, W.J. Weber, "Quantification of actinide-radiation damage in minerals and ceramics," Nature 445 (2007).*
2. *I. Farnan, H. Cho, W. Weber, R.D. Scheele, N.R. Johnson, A.E. Kozelisky, "High-resolution solid-state nuclear magnetic resonance experiments on highly radioactive ceramics," Rev. Sci. Instrum., 75 (2007).*
3. *G. Wallez, P.E. Raison, N. Dacheux, N. Clavier, D. Bykov, L. Delevoye, K. Popa, D. Bregiroux , A.N. Fitch, R.J.M. Konings, "Triclinic–Cubic Phase Transition and Negative Expansion in the Actinide IV (Th, U, Np, Pu) Diphosphates," Inorg. Chem., 51 (2012).*

This article was contributed by R. Natarajan, V. Vijayakumar, V. Sundararaman, and A. Ravisankar of the Reprocessing Group, Indira Gandhi Centre for Atomic Research, Kalpakkam, India.

Plutonium-rich Fast Reactor Spent Fuel Reprocessing in CORAL and Beyond

The pilot plant, CORAL (compact facility for reprocessing of advanced fuels in lead cells), was designed and commissioned at the Indira Gandhi Centre for Atomic Research (IGCAR), for reprocessing the spent mixed carbide fuels of the fast breeder test reactor (FBTR). This plant has been operating since 2003, providing valuable experience with reprocessing high burn-up fuels containing high plutonium concentrations (Fig. 1). The objective of this facility is to demonstrate the aqueous reprocessing process flowsheet for high burn-up and rich plutonium-bearing fuels with the required recoveries and purities. This would validate the design of several pieces of process equipment and the design features of the commercial plants.

The CORAL facility forms the second phase of four phases of the technology development of Indian fast reactor fuel reprocessing, which are as follows:

Phase I: Development phase, which broadly consists of process formulation, validation, design, and development of equipment.

Phase II: Design, construction, and operation of CORAL.

Figure 1. A view of the operating area of CORAL.

Phase III: Design, construction, and operation of the demonstration fast reactor fuel reprocessing plant (DFRP) to gain experience in fast reactors fuel reprocessing with high availability factors and plant throughput.

Phase IV: Design, construction, and operation of a commercial fuel reprocessing plant (FRP) for reprocessing of prototype fast breeder reactor (PFBR) fuel.

The process flowsheet used in CORAL is based on the PUREX process, that was adapted for high-plutonium-bearing fuels. The chop-leach process is deployed with dissolution of the spent fuel in concentrated nitric acid under refluxing conditions. The dissolver has provision for electrolytic oxidation. Three cycles of solvent extraction with electrolytic partitioning in the third cycle is provided in the plant. The solvent is 30% tributyl phosphate in normal paraffin diluent. Reconversion of plutonium is planned using the oxalate process while reconversion of uranium is based on ammonium hydroxide. The spent fuel subassembly from FBTR is dismantled in another hot-cell facility using laser cutting. The fuel pins are drawn from the hex-can and transferred to the CORAL facility in a shielded cask (Fig. 2).

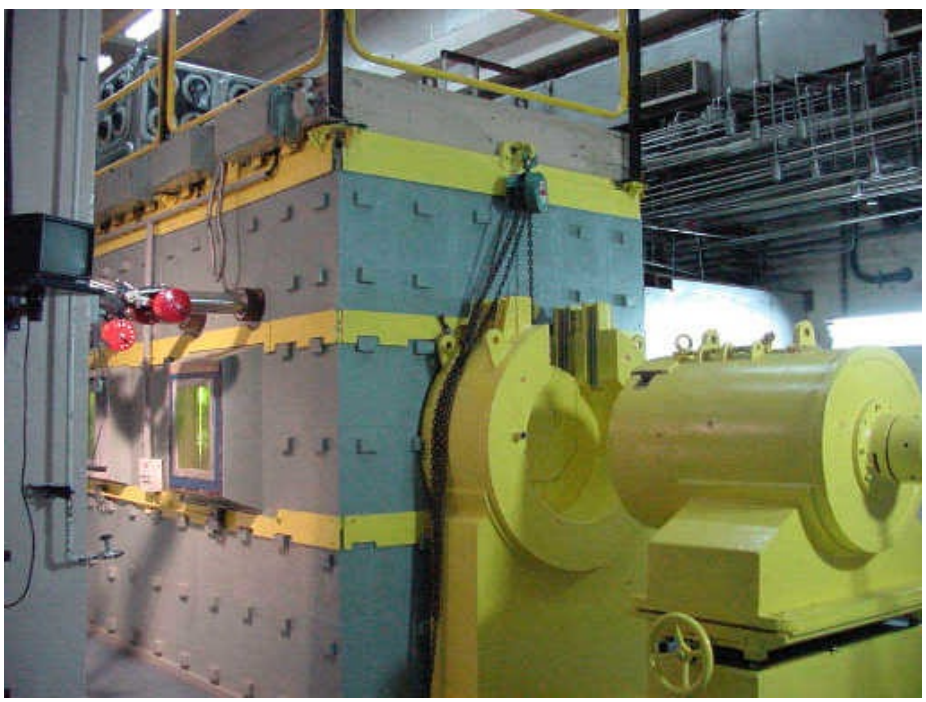

Figure 2. Shielded cask containing the fuel pins from the dismantled spent fuel assembly aligned with the CORAL hot cell.

The CORAL facility has a lead-shielded stainless steel containment box where the process equipment, such as the chopper, dissolver, centrifuge, and centrifugal extractors are kept to enable remote operation and maintenance. Contact maintenance is carried out in a blister box aligned to the containment box. All the process vessels are designed to meet the criticality safety considerations for handling a high plutonium inventory. The specially designed in-cell cranes and master-slave manipulators aid in remote operations and maintenance within the α-containment box. Viewing windows enable personnel to carry out remote maintenance when required.

The CORAL containment box was commissioned with a leak rate of less than 0.5%/hr while operating to reduce the leak of radioactive gases in case of negative pressure during an emergency situation. The facility was "hot" commissioned in December 2003 with the approval of the Atomic Energy Regulatory Board (AERB) for reprocessing very low burn-up spent fuel. Since then many reprocessing campaigns with progressively increasing burnups and reduced cooling periods have been successfully accomplished in this facility. Safety clearance from the AERB was required before every stage of reprocessing the fuel with increased burn-ups and reduced cooling times.

For the last 9 yrs, the operation of this unique facility has provided invaluable data for the design of future facilities in various areas such as process, equipment, and remote hot-cell equipment. Areas requiring improvement have been identified based on this experience, such as decreasing radiation exposures and waste generation and reducing the number of operations.

Several pieces of equipment such as the chopper, dissolver, centrifuge, and centrifugal extractor unique to fast reactor spent fuel reprocessing have been developed and tested in CORAL. Because the fast reactor fuel pins are thin, to avoid crimping, single-pin choppers have been developed (Fig. 3). Chopping operations in CORAL consists of fuel-pin feeding by a stepper motor, followed by fuel-pin gripping and chopping operated by pneumatic actuators. The alignment of the magazine, which houses the pins, is by a pneumatic actuator, which feeds the fuel pins one after another. The movement of the pin for a prespecified length is ensured by the stepper motor. The chopped pieces fall directly into the dissolver basket through the duct connecting the chopper and dissolver. The operation of the single-pin chopper in CORAL is very satisfactory; the design was adopted for the future plants with some additional features for increasing the throughput.

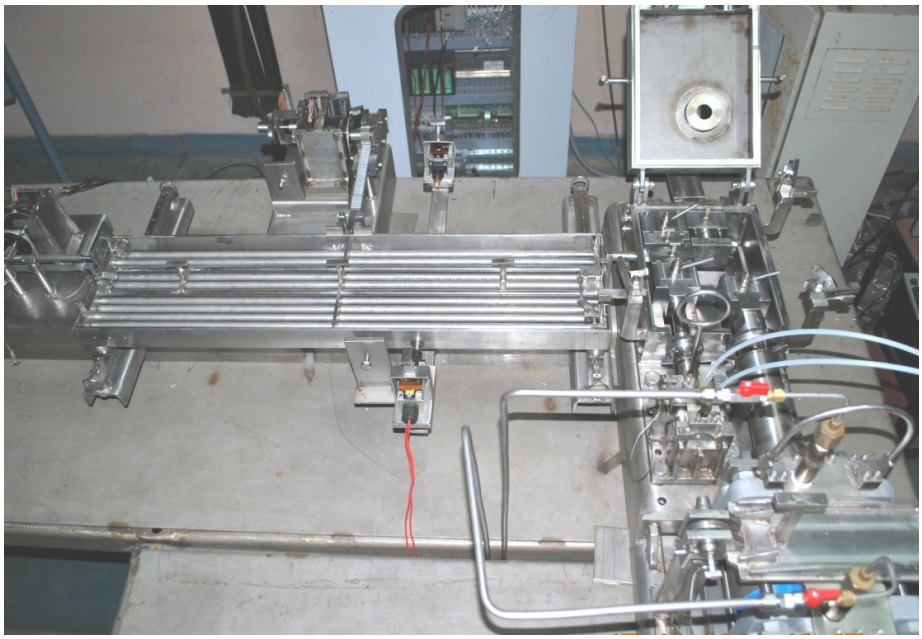

Figure 3: A single-pin chopper for the DFRP undergoing testing.

The dissolution of high plutonium-bearing carbide and oxide fuels of fast reactors require higher nitric acid concentrations and a temperature of about 100 °C–110 °C to ensure complete dissolution. In order to withstand the highly corrosive environment prevalent in the dissolver, titanium and zirconium have been identified as the appropriate materials for construction. In CORAL, titanium Grade-2 material was selected as the material of construction based on various considerations such as availability. Visual inspection of the dissolver after several dissolution campaigns revealed satisfactory performance. The same material has been chosen for the future plants as well. To reduce the dissolution time, additional features, such as an agitator for hulls, are incorporated in these designs. It has been observed that the dissolver solution does not contain any detectable undissolved solids although some fine black particles are occasionally present. Based on operating experience, electrolytic oxidation is unnecessary; extended dissolution under refluxing condition is sufficient. Since the dissolution behavior of mixed oxides (MOX) could be different, the option of oxidative dissolution has not been eliminated in the design of these dissolvers for future plants. The experience with centrifuge clarification for the removal of fine particles is inconclusive due to maintenance-related issues in CORAL. Since MOX fuel dissolution is not presently available and because the limited literature available with high Pu-bearing MOX spent fuel dissolution indicates that fine particles containing noble metal alloys may be present, the centrifuge clarification will be incorporated in the future plants.

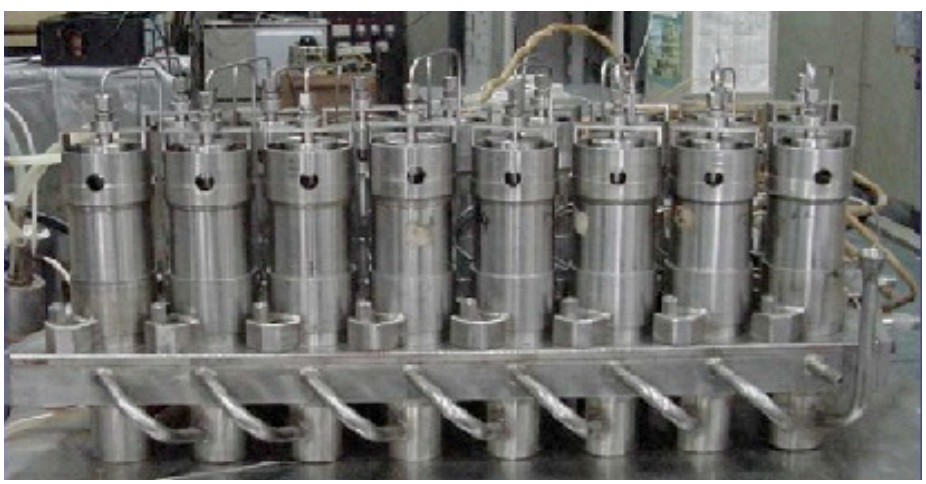

Figure 4. A staged annular centrifugal extractor in CORAL.

Because the success of the PUREX process for fast reactor fuel reprocessing primarily lies in reducing radiation damage to the solvent, R&D on low-residence-time contactors such as centrifugal extractors is pursued at IGCAR. Annular centrifugal extractors (ACE) are used in all the cycles of solvent extraction in CORAL (Fig. 4). The CORAL operating experience has provided understanding of various aspects of the intricate designs of the bowl and the electrical motors. Motor designs have been extensively evaluated in this facility in order to improve the reliability of operation and the timely detection of failures. Presently, capability exists for designing ACE

for different systems (U-Pu, U-Th, and WPA-DEPHA-TBP systems) and varying capacities with bowl sizes ranging from 25 mm to 1000 mm.

As the performance of the electrolytic partitioning system in CORAL was not satisfactory, partitioning with oxalate precipitation was adopted during the operation of the plant. The purity requirements of the plutonium product could be met by this process, but uranium purity requirements could not be satisfied. Hence, in future plants, alternate partitioning methods would be adopted based on the R&D currently in progress.

The several campaigns of reprocessing with the spent fuels of FBTR containing up to 70% plutonium fuel completed in the CORAL facility has demonstrated the feasibility of meeting the exacting requirements of fast reactor fuel reprocessing based on the PUREX process. The cooling period of the 155 GWd/t burn-up FBTR mixed carbide fuel has been fixed as 2 years due to various considerations; R&D efforts are in progress to reduce this time further and address the associated issues.

Based on the experience in CORAL, where the required decontamination factors could be achieved with single solvent extraction cycle, further studies are in progress to explore the modifications that may be required in the solvent extraction flowsheet while handling fuels with shorter cooling times. One of the important R&D activities is reducing the number of solvent extraction cycles while still attaining the required purity requirements as this would reduce the waste volumes.

The difficulties that one would face while designing the solvent extraction flowsheet for plutonium-rich, high burn-up fast reactor fuels with short cooling times would be achieving the required decontamination factors for the fission products zirconium and ruthenium. This is primarily because their distribution ratios are reasonably high and their extraction behavior is complex. The fact that they behave quite the opposite with respect to acidity makes it difficult to achieve the required separation by acid scrubbing. The design is intended to achieve the required decontamination factors for both of these very different fission products in a single cycle, a challenging job as their extraction behaviors are exactly opposite. A flowsheet with dual scrub; one for removing ruthenium, which requires higher acidity, and another for removing zirconium, which has a lower acidity, was formulated using the computer modeling code PUSEP (ver-2) and demonstrated under simulated conditions. The conditions for third-phase formation due to possible unexpected conditions were also identified. The concept of dual scrub is unique and has not been followed in conventional PUREX flow sheets. The other important ongoing activity is the development of a partitioning flowsheet that was formulated and demonstrated. In this work, the stoichiometric requirement of U(IV) for achieving the required separation between uranium and plutonium was reduced to just 1.5, while conventionally 5 to 7 times is required to compensate for the use of U(IV) because of parasitic reactions. Another safety-related problem that was addressed was the removal of dissolved

solvent in the waste solution before evaporation to reduce the risk of "red-oil" formation and for purification of the solvent for recycling.

Estimation of the amount of plutonium in the hulls left out after dissolution is very important for various safety considerations. A method based on tagging with ^{144}Ce to assay the plutonium has been standardized and successfully deployed. This method overcomes the difficulties due to the ^{60}Co activation product since the γ energy is well separated (Fig. 5). This method is not feasible if the spent fuel is cooled for more than 5 yrs, and so this approach is ideally suited for fuels with short cooling times.

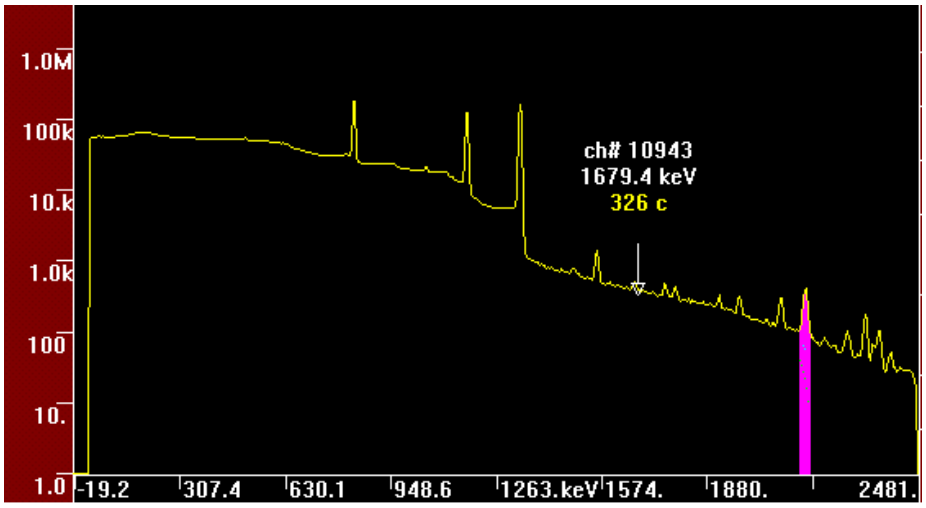

Figure 5. Typical γ spectrum of fast reactor spent fuel hulls with the γ peak of ^{144} Ce highlighted in magenta.

R&D is also in progress for carrying out in-service inspection and to resolve material-related issues for increasing the life of reprocessing plants. An exclusive laboratory for measurement of thermo-physical properties required for solvent extraction process modeling has been set up. Analytical techniques, such as monitoring the concentration of plutonium online and methods for timely detection of third phase formation that would aid in the timely detection of off-normal and unsafe plant operation are also being pursued.

The operating experience of CORAL and the beneficial R&D programs formulated establishes not only adapting the proven PUREX process for plutonium-rich short-cooled fuels but also in establishing the hot-cell designs for incorporating the O&M (operation and maintenance) features for reliable and safe operation of the plant.

The CORAL operating experience led to the design of equipment and systems for the demonstration plant, DFRP. The primary design objectives of this plant are the establishment of high plant throughputs, high recoveries, and reduced waste volumes. In this plant, not only mixed carbide, but also mixed oxide fuels of FBTR will be reprocessed. The spent fuels from

the PFBR reactor, which is currently under construction at Kalpakkam, will also be demonstrated in this plant. DFRP is in an advanced stage of construction with vital equipment being installed, such as the single-pin chopper, dissolver, centrifuge, centrifugal extractors, and sampling systems, that were designed and fabricated based on CORAL operational feedback.

With the pilot plant in operation, the demonstration plant under erection, and the prototype plant under design, the Indian nuclear power program is poised for exponential growth as it introduces fast reactors and the associated fuel cycle.

Further reading:

1. *R.V. Subba Rao, M. Venkataraman, R. Natarajan, Baldev Raj, "Operating Experience of fast reactor spent fuel reprocessing facility CORAL," Proceedings of GLOBAL 2009 symposium, paper 9126, 172-178, Paris (2009).*
2. *G. Santosh Kumar, K.S. Vijayan, S. Ganesh, P. Govindan, M.C. Devarajan, S.V.Mohan, R.V. Subba Rao, M. Venkataraman, R. Natarajan, "Evaluation of fission products decontamination by direct oxalate precipitation Plutonium," Proceedings of DAE-BRNS Biennial Symposium SESTEC, 313-14 (2010).*
3. *R. Natarajan, N.K. Pandey, K. Dhamodharan, R.V. Subba Rao, V. Vijayakumar, U. Kamachi Mudali, "Empirical Modeling for Distribution of Zirconium and Ruthenium in Nitric Acid – Tri-butyl phosphate/ Normal Paraffin Hydrocarbon," Sep. Sci. & Tech. (Communicated).*
4. *R. Natarajan, N.K. Pandey, V. Vijayakumar, R.V. Subbarao, "Modeling and Simulation of Extraction Flowsheet for FBR Fuel Reprocessing," ATALANTE 2012–International Conference on Nuclear Chemistry for Sustainable Fuel Cycles, Procedia Chemistry 7, 302-308 (2012).*
5. *V. Reshmi, N.K. Pandey, R. Sivasubramanian, S. Ganesh, M.K. Ahmed, U. Kamachi Mudali, R. Natarajan, "Process modeling of in-situ Electrochemical Partitioning of Uranium & Plutonium in Purex Process: Benchmark Results with Uranium Reduction," Desalination & Water Treatment, v. 38, 29-39 (2012).*

The Optical Properties of the Plutonium/Plutonium Oxide Thin Film System

This article was contributed by David L. Pugmire, Franz J. Freibert, and Joseph P. Baiardo, Los Alamos National Laboratory Materials Science and Technology Division.

The oxidation of plutonium continues to be an area of considerable interest. Corrosion rates of Pu, a reactive metal, and the characteristics of the ever-present oxide layer have significant implications for Pu production, use, storage, and disposition. The nature of oxide film has historically been considered an overlayer of the cubic dioxide (PuO_2) on the metal substrate, based largely on X-ray diffraction analysis of thick oxide films. Using thermodynamic arguments, it has been postulated that a thin layer of the cubic sesquioxide (α-Pu_2O_3) should be present at the interface between the oxide film and the metal substrate. For these reasons, PuO_2 has historically been the material of interest to anyone studying the surface properties of plutonium metal. However, our recent work on the very initial stages of plutonium oxidation under the ideal conditions of ultra-high vacuum have indicated that the oxide formed when Pu is exposed to O_2 is not crystalline and does not consist of discrete layers. Here we report on results from our preliminary studies using spectroscopic ellipsometry (SE) of room-temperature atmospheric corrosion of plutonium metal. Spectroscopic ellipsometry is a powerful tool that has been used for decades to measure the thickness of films, including oxide films grown on metal substrates.

For studies presented here, a plutonium metal sample (δ-stabilized Pu/Ga alloy) was polished in an inert glovebox to remove all oxide from the surface. Growth of an oxide layer by exposure of the sample to laboratory air was monitored with SE for 2 months. The oxide thickening results over time are shown in Fig. 1, with individual measurements represented by black squares. The top graph shows the results obtained during the first hour of exposure; by the time the first measurement was made, 12 min after polishing, an oxide film nearly 23-nm thick had grown. After an hour, the oxide film gradually increases in thickness to approximately 27 nm. The bottom graph shows the thickness of this oxide at longer exposure times, reaching 85 nm after 60 days of exposure to air. The oxidation of δ-Pu under relatively dry conditions, such as those employed here, have been shown to result in an oxide film that is quite protective against further oxidation, occurring at a rate of 0.02 nm/hr, identical to the rate observed here after two months' exposure. The oxide thickness data measured here does not fit well with the more common linear or parabolic growth models, but does fit quite well by an inverse logarithmic function (black line in Fig. 1, very fast initial growth followed by rapid reduction in rate), perhaps also indicating this protective behavior.

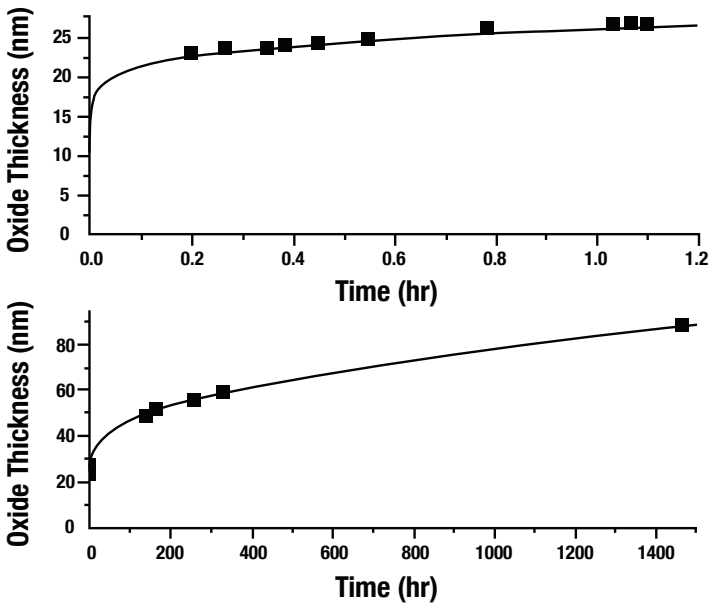

Figure 1. Oxide thickening results over time.
- Top graph: Results during first hour of exposure.
- Bottom graph: Thickness of oxide at longer exposure times.

In addition to film thickness, analysis of data obtained with SE can also provide information on a host of optical properties related to the electronic structure, such as the index of refraction and dielectric constants. The optical constants determined here for the oxide that grows upon exposure of plutonium to air at room temperature are vastly different from what has previously been measured for a crystalline PuO_2 film, and are not at all what would be expected for polycrystalline PuO_2. This may not be entirely unexpected based on our earlier work that indicated this thin oxide grown on plutonium metal at room temperature is likely not the crystalline form of PuO_2 that is most often used to describe the film. Additionally, historical work on the low-temperature corrosion of metals would argue that any thin, protective film such as that which grows on Pu at room temperature in dry air should not be crystalline. This has significant consequences for any work aimed at understanding the chemical properties of plutonium surfaces.

The presence of an oxide film on plutonium not only affects the storage and use of the metal, but can also have significant effects on any scientific or diagnostic measurements, particularly those using optical techniques. The index of refraction (n) and extinction coefficient (k) of plutonium and the oxide grown by exposure to air at room temperature discussed here can be used to calculate various optical characteristics of the system such as the spectral reflectivity. This is demonstrated in Fig. 2, which shows the calculated spectral reflectivities for 40- and 60-nm-thick oxide films on plutonium metal. The spectra show that the reflectivity drops to 0% at wavelengths of 415 nm (purple light) for the 40-nm-thick film and 570 nm (yellow light) for the 60-nm-thick film. These reflectivity minima are important because if purple light, 415 nm, is not reflected from the 40-nm-thick film, the surface would then be expected to appear yellow or gold (opposite color to purple on a color wheel) when viewed under white light. Correspondingly, the 60-nm-thick film would be expected to appear

purple. These results confirm the earliest single-wavelength ellipsometric studies of plutonium oxidation and provide an easy-to-use visual correlation between the colors commonly observed for Pu surfaces and the thickness of the oxide.

Optical diagnostics are critical to the measurement of surface velocity in shock experiments and the derivation of properties during dynamic loading of plutonium, which depend on the reflectance of rapidly moving surfaces. One such technique, VISAR (velocity interferometer system for any reflector), relies on the reflectivity of light with a wavelength of 532 nm from the plutonium/plutonium oxide surface, needing at least a 10% reflectivity for reliable results. As shown in Fig. 2 and discussed above, the reflectivity vs wavelength calculated from the n and k values determined with SE reveal an extreme sensitivity of reflectance to oxide thickness from the near-UV to visible wavelengths of light. It is also possible to calculate the reflectivity vs oxide thickness for a given wavelength. Figure 3 shows the reflectivity of 532-nm light as a function of Pu oxide thickness. It can be seen that at a thickness of just over 35 nm, the reflectivity drops below the critical value of 10% for this technique. As shown in Fig.1, an oxide on plutonium of this thickness is achieved in less than one day of exposure to dry air. Even "inert" environments, such as the typical inert glovebox (approx. 1% O_2) used for plutonium handling, will likely result in similar oxide film thicknesses over similar exposure times, as previous studies of plutonium oxidation with much lower oxygen partial pressures (0.01%) show a film thickness of nearly 30 nm after 7 hrs exposure. Figure 3 also shows that after the oxide thickens to approximately 80 nm, the surface begins to reflect the necessary 10% for this technique. However, Fig. 1 also shows that a rather significant exposure

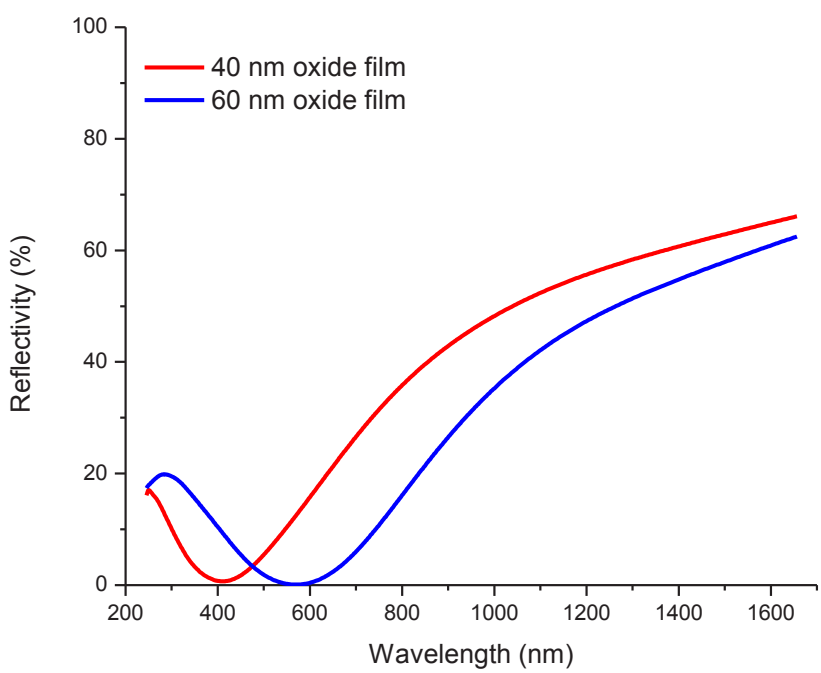

Figure 2. Calculated spectral reflectivities 40- and 60-nm-thick oxide films on plutonium metal.

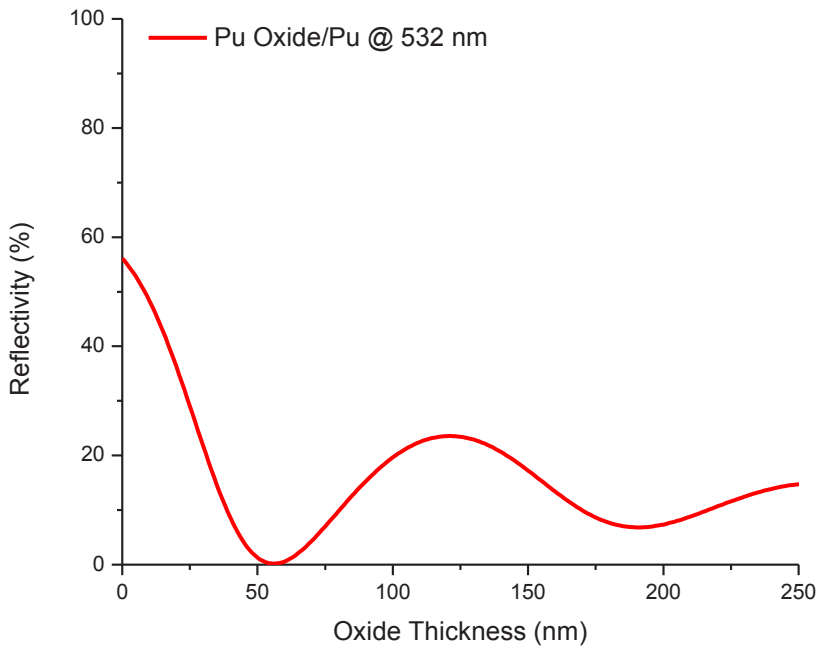

Figure 3. Reflectivity of 532-nm light as a function of Pu oxide thickness.

time is required to achieve this thickness. This presents a potential problem for the application of VISAR on plutonium surfaces.

The results presented here highlight how powerful SE can be in developing an understanding of the oxidation of plutonium and the optical properties of plutonium surfaces. We are also using SE, and the data it provides, to gain insights into the complex electronic properties of plutonium metal. As described in this article, an understanding of the optical properties of plutonium surfaces allows for accurate determination of the spectral reflectivity. Spectral emissivity can be determined from reflectivity via a simple relation, and subsequently used to determine the temperature of the surface. With future work, the data provided by SE may greatly enhance our ability to make accurate, in-situ, temperature measurements improving the equation of state determination for plutonium from dynamic experiments.

Further Reading:

1. *H.G. Garcia Flores, P. Roussel, D.P. Moore, D.L. Pugmire, "Characterization and stability of thin oxide films on plutonium surfaces," Surface Science, 605 (2011) 314-320.*
2. *J.M. Haschke, T.H. Allen, L.A. Morales, "Surface and corrosion chemistry of plutonium, " Los Alamos Science, 26 (2000) 252-273.*

Plutonium Futures Conference

Renaissance Hotel, Las Vegas, NV • September 7-12, 2014

The
Plutonium Futures Conference
provides
an international forum
for the discussion of current research on the physical, chemical, and mechanical properties of plutonium and other actinides.
By bringing people of diverse disciplines together, the conference aims to
enhance the dialogue among scientists and engineers
on the
fundamental properties of plutonium and their technological consequences.

The conference will include discussions of condensed matter physics, materials science, metallurgy, surface science, corrosion, colloids, actinide chemistry, detection and speciation analysis, environmental science, fuel-cycle issues, and advanced nuclear fuels.

A tutorial session will be held on the opening Sunday afternoon.

It will be the eighth conference in the series, which was initiated by Los Alamos National Laboratory in 1997. Previous conferences have been held in

Santa Fe, New Mexico – 1997 and 2000 • Albuquerque, New Mexico – 2003
Asilomar, California – 2006 • Dijon, France – 2008
Keystone, Colorado – 2010 • Cambridge, United Kingdom – 2012

The 2014 conference is co-sponsored by Lawrence Livermore and Los Alamos national laboratories and the American Nuclear Society (ANS).

Kerri Blobaum and Scott McCall are the general and program chairs, respectively. Information on registration, call for papers, and lodging will be available through the ANS webpage.

Questions or requests to be added to the conference mailing list should be sent to

Kerri Blobaum (blobaum1@llnl.gov) or Scott McCall (mccall10@llnl.gov).

Prepared by LLNL under Contract DE-AC52-07NA27344.

Pages 26 Photos:

Top left: Robert Böhler (EC, JRC-ITU) (center) was the Physics winner (Institute of Physics-sponsored prize for "Vibrational spectroscopy of plutonium dioxide". © British Crown Owned Copyright 2013/AWE

Top right: Fanny Lalire (CEA) (right) was the Materials winner (Armourers and Braziers sponsored prize) for "Kinetic study of delta to alpha' isothermal martensitic transformations in PuGa1at%".
© British Crown Owned Copyright 2013/AWE

Center left: Jammu Ravi (Indira Gandhi Centre for Atomic Research) (left) was the Chemistry winner (Royal Society of Chemistry-sponsored prize) for "Unsymmetrical diglycolamides for minor actinide partitioning". © British Crown Owned Copyright 2013/AWE

Center right: Ségolène Cocollomb (CEA) (center) was the Nuclear Fuel Cycle winner (Institute of Materials, Mineralogy and Mining-sponsored prize) for "Influence of oxygen potential on microstructure and interdiffusion in (U, Pu)O2 fuel".
© British Crown Owned Copyright 2013/AWE

Bottom left: The conference was chaired by (from left) Thomas Fänghanel (JRC-ITU), Claude Guet (CEA), and David Geeson (AVE). Photo by D. Hobart

Bottom center: An overhead view of the Pu Futures student poster session. Photo by D. Hobart

Bottom right: Sir Mark Welland addresses Pu Futures attendees. Photo by D. Hobart

Page 27 Photos (Left-top to bottom):

Neil Seagrave (AWE) (left) speaks with Sig Hecker (CISAC, Stanford Univ.) during the conference poster session. Photo by D. Hobart

Alexey V. Mirmelstein, VNIITF (left) speaking with Paul Potter (AWE) and Boris Nadykto, VNIITF (left).
Photo by D. Hobart

Registration staff greets and supplies conference attendees. Photo by D. Hobart

While in the UK, attendee David Hobart (LANL) visited his ancestral family home, Blickling Hall, a National Trust property in Aylsham, Norfolk. Photo by D. Clark

right: Queens' College, University of Cambridge, was a regal setting for the conference reception and dinner.
© British Crown Owned Copyright 2013/AWE

Back cover photo: A view of Clare College. University of Cambridge

ACTINIDE RESEARCH QUARTERLY
is published by Los Alamos National Laboratory and is a publication of the Glenn T. Seaborg Institute for Transactinium Science, a part of the National Security Education Center. ARQ highlights research in actinide science in such areas as process chemistry, metallurgy, surface and separation sciences, atomic and molecular sciences, actinide ceramics and nuclear fuels, characterization, spectroscopy, analysis, and manufacturing technologies.

Address correspondence to:
Actinide Research Quarterly
c/o Editor
Mail Stop B260
Los Alamos National Laboratory
Los Alamos, NM 87545

ARQ can be read online at:
www.lanl.gov/arq

If you have questions, comments, suggestions, or contributions, please contact the ARQ staff at:
arq@lanl.gov or (505) 667-0392

National Security Education Center
David L. Clark
Director

Scientific Advisors, Seaborg Institute
Albert Migliori,
Seaborg Institute Director
Gordon D. Jarvinen,
Seaborg Institute Deputy Director

Technical Editors
David Hobart
Gordon D. Jarvinen

Editor
Sue King

Contributing Editors
Eileen Patterson
Susan Ramsay

Designers/Illustrators
Kelly L. Parker
Leslie A. Sandoval

Photo Support
David Hobart
Andrew Cox

Printing Coordinator
David Van Etten